



MIT
SEA
GRANT
PROGRAM

CIRCULATING COPY
Sea Grant Depository

A FLUME FOR THE STUDY OF CONTAINED OIL SLICKS

By

Jerome Milgram

Robert Van Houten



Massachusetts Institute of Technology

Cambridge, Massachusetts 02139

Report No. MITSG 77-19

July 1977

A FLUME FOR THE STUDY OF
CONTAINED OIL SLICKS

by

Jerome H. Milgram
and
Robert Van Houten

July, 1977

Sea Grant Program

Massachusetts Institute of Technology

Cambridge, Massachusetts 02139

Report No. MITSG 77-19
Index No. 77-319-Nom

Table of Contents

<u>Section</u>	<u>Title</u>	<u>Page</u>
1	INTRODUCTION.....	1
2	OVERALL FLUME DESIGN.....	4
3	INDIVIDUAL FLUME COMPONENTS.....	7
	Test Section.....	7
	Overall Flume Structural Support.....	11
	Weir Section.....	13
	Sump Tank.....	19
	Diffuser.....	24
	Turning Vane Section.....	25
	Stilling Section.....	25
	Contraction.....	29
4	OPERATIONAL TESTS.....	29
	Flume Calibration.....	29
	Flow Uniformity.....	34
	Turbulence and Vibration Levels.....	37
	REFERENCES.....	41

Illustrations

<u>Table</u>	<u>Title</u>	<u>Page</u>
1.	Weir Flows and Test Sections Flow Speeds for Various Weir Setting.....	17

<u>Figure</u>	<u>Title</u>	<u>Page</u>
1.	Sketch of Typical Flume Test Section Geometry for an Experiment with a Contained Oil Slick..	3
2.	Isometric Transparent Cut-away View of Flume..	5
3.	Plane Views of Flume.....	6
4.	Test Section Drawing.....	8
5.	Isometric Drawing of Main Structural Supporting Elements.....	12
6.	Geometry of Tilting Weir Section.....	15
7.	Weir Flows Versus Opening Beneath Weir.....	18
8.	Construction Drawing of Sump Tank.....	20
9.	Drawing of Mold Shape Used for Nozzle Construction.....	23
10.	Flume Diffuser.....	26
11.	Turning Vane Section.....	27
12.	Stilling Section.....	28
13a.	Top View of Contraction.....	30
13b.	Side View of Contraction.....	31
14.	Water Surface Speed Calibration.....	33
15.	Survey of Flow Speed (1 ft/sec).....	35
16.	Survey of Flow Speed (2.5 ft/sec).....	36
17.	RMS Velocity Fluctuations Versus Mean Flow Speed Beneath Free Surface Effects.....	40

Authors

Jerome Milgram is a professor in the Massachusetts Institute of Technology Department of Ocean Engineering.

Robert Van Houten is a Research Associate in the Massachusetts Institute of Technology Department of Ocean Engineering.

Acknowledgments

This work and the construction of this flume were supported in part by The National Science Foundation under grant number ENG 72-03943 A04 and in part by the M.I.T. Sea Grant program with support from the Office of Sea Grant in the National Oceanic and Atmospheric Administration, U.S. Department of Commerce, through grant number 04-6-158-44007, and from the Massachusetts Institute of Technology. The U.S. Government is authorized to produce and distribute reprints for governmental purposes notwithstanding any copyright notation that may appear hereon.

The Sea Grant Information Center maintains an inventory of Sea Grant publications, and a descriptive catalog of these works can be obtained free of charge upon request. We invite inquiries to:

Sea Grant Information Center
M.I.T. Sea Grant Program
Room 5-331
Massachusetts Institute of Technology
77 Massachusetts Avenue
Cambridge, Massachusetts 02139

1. INTRODUCTION

The hydrodynamics associated with a contained, and nearly stationary, oil layer above a moving water current are far from completely understood. As an aid in studying this hydrodynamical problem, we have designed and built a special flume at the Ocean Engineering Department of M.I.T. Design requirements for water flumes are well documented (see e.g.; Orkeny, 1955; Steele, 1962; or Preston, 1966). However, there are several special requirements for a flume to be used for the study of contained oil pollution which lead to a specialized device, called an oil layer flume, that is useful for studying many other hydrodynamic problems as well.

A major influence on optimum flume geometry results from the high length/depth ratio of typical oil layers contained by a boom in a current (see e.g.; Miller, Lindenmuth, and Altman, 1972). A typical length/depth ratio is 200, and even higher ratios are common. Several important entrainment and dispersion mechanisms leading to the failure of an oil boom to contain the oil in a current are strongly influenced by the gravitational densimetric Weber number, $Tg\Delta/\rho_w U^4$, where

T = oil-water interfacial tension,

g = acceleration due to gravity,

ρ_w = water density,

ρ_o = oil density,

U = current speed, and

$$\Delta = \frac{\rho_w - \rho_o}{\rho_w}$$

Since only a very limited range of interfacial tensions are obtainable, and since $U \sim T^{1/4}$ for a scale model experiment with fixed density ratio, current speeds in an experiment must be nearly equal to full scale speeds.

A scale model experiment requires the full scale value of the densimetric Froude number, $U/\sqrt{g\Delta d}$, where d is a characteristic contained oil slick depth. Therefore, essentially full scale lengths and depths are required in the experiments.

In our case, and in most other circumstances as well, it is impractical to build a flume as long as a typical full scale contained slick. Therefore, the flume length will limit the range and importance of possible experiments. A major consideration for an oil layer flume is maximum possible test section length. A typical test section experimental geometry is shown in Figure 1.

All previous flume experiments on contained oil layers have been done in flumes having freestream rms turbulence levels of at least several percent of the mean flow speed. The role of this turbulence on apparent instabilities of the oil-water interface is unknown. Since the interface responds to turbulent pressure fluctuations, the turbulence can mask natural instabilities. The apparent interfacial instabilities lead to containment failure of pollution control devices so that they are of considerable interest. Studying them is facilitated by a low level of freestream turbulence. As a result, emphasis must be placed on achievement of a low turbulence level in the design of an oil layer flume.

A flume experiment can be an approximate model only of a "two-dimensional" section of a contained oil slick. The width of the flume is necessarily small in comparison to the slick length so that transverse variations must be kept to a minimum. As a result, special emphasis must be placed on lateral uniformity of the flow in a flume. Vertical uniformity is less important and the requirements on it are similar to the requirements on the vertical uniformity for most other flumes.

During operation, some oil droplets will become entrained in the water beneath the oil. These droplets will circulate

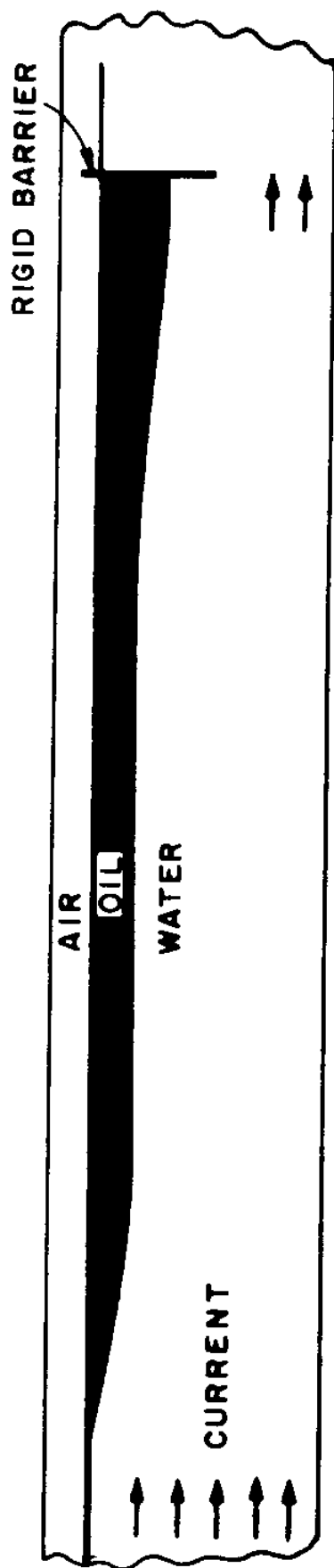


FIGURE 1. Sketch of Typical Flume Test Section Geometry for an Experiment with a Contained Oil Spill.

through the flume. It is desirable to minimize further splitting of these droplets since microscopic droplets make the water cloudy and are difficult to separate out of the water. Therefore, the pump or impeller of the flume must be of a type which minimizes fine droplet emulsification.

When the flume is shut down, most of the oil must be removed and put into storage tanks. Inevitably, some oil will remain in and on the water and on the flume surfaces. Much of this oil eventually ends up on the water surface and it is desirable to be able to remove it from the water surface over an extended period of time. The handling of the major part of the oil to be initially removed and the smaller quantity of oil to be removed over an extended period of time are other special design considerations.

It is well known that the entrainment of oil droplets from a contained slick into the flowing water beneath it occurs at current speeds above 2.5 ft/sec. Therefore, the design operating current speed range for our flume was chosen as 0 to 4 ft/sec. The nominal operating fluid depth, h , was chosen as 1.5 feet for reasons described subsequently. Thus, the critical flow speed (\sqrt{gh}) is 7 ft/sec and the operating flume Froude number range is 0 to 0.6. Therefore, a design for totally subcritical operation is required.

2. OVERALL FLUME DESIGN

Meeting the special requirements described in Section 1 has led to a basic design that is a "hybrid" of the sump type of flume and the "wind tunnel circuit" type of flume (see Preston, 1966, for an explanation of basic flume types). The overall geometry is shown in Figures 2 and 3. The fluid from the test section spills into a sump tank through a combination weir having fluid passing over it and under it. The purposes of the sump tank are to remove air entrained in the fluid and

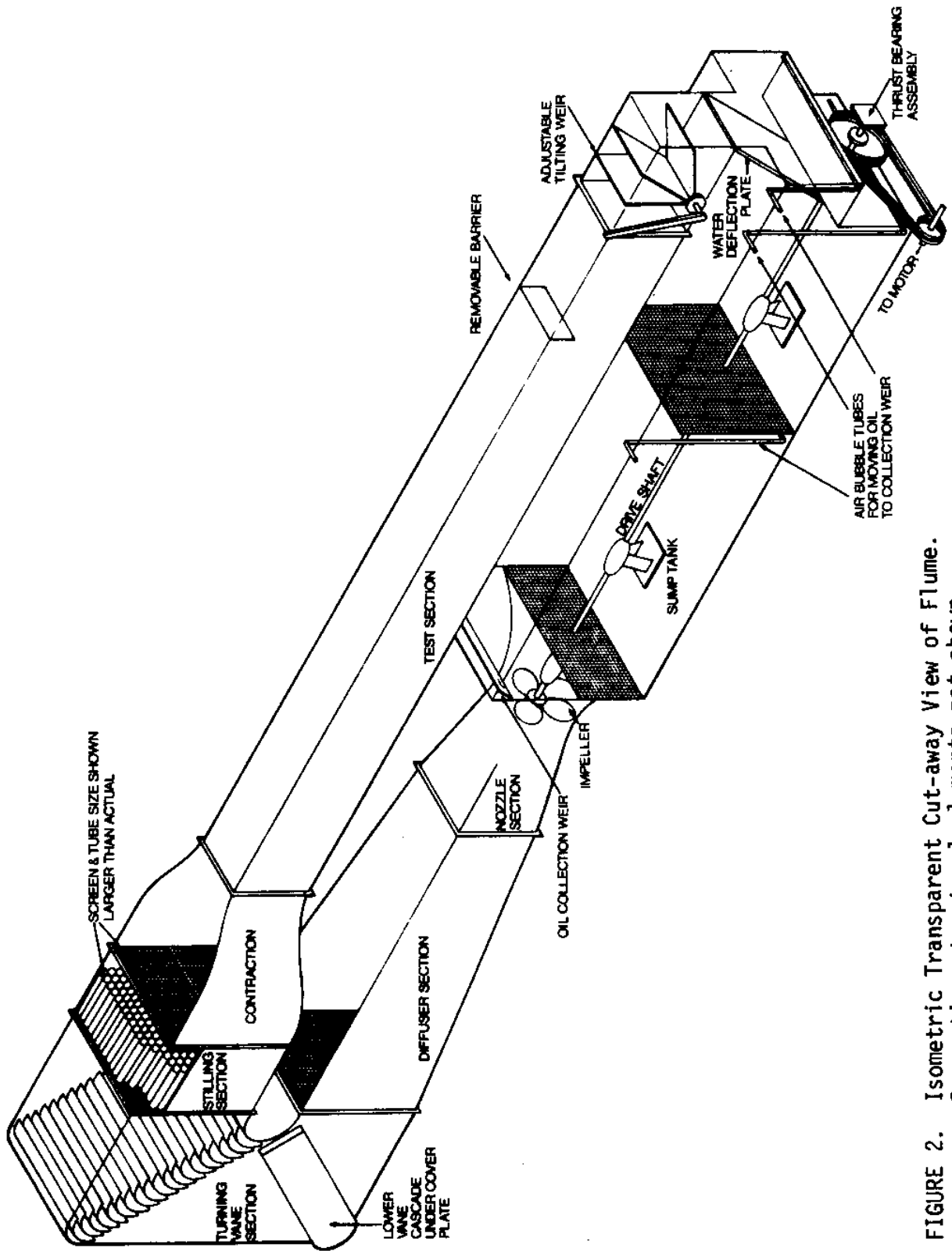


FIGURE 2. Isometric Transparent Cut-away View of Flume.
Supporting structural elements not shown.

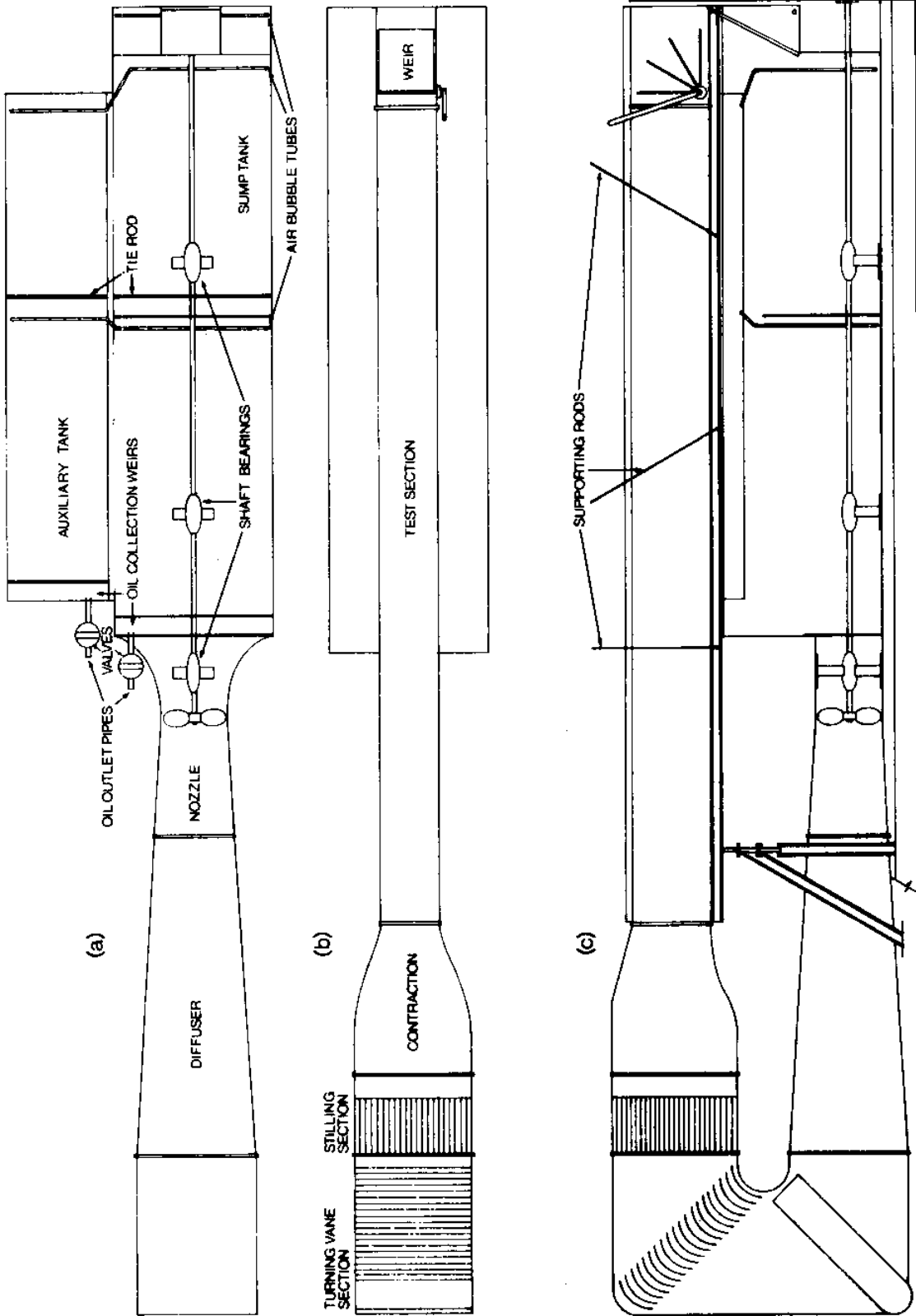


FIGURE 3. Plane Views of Flume.
 (a) Plan view of lower branch.
 (b) Plan view of upper branch.
 (c) Elevation.

to collect most of the oil that is not contained in, or removed from, the test section. The remainder of the circuit is of the "wind tunnel type". From the sump tank, the flow passes through a contracting and then diverging nozzle section. The minimum area portion of the nozzle has a circular cross section and surrounds the flume impeller which is of the ducted propeller type. From the nozzle section, the flow passes through a diffuser in which the flow area is expanded. The flow is then turned through ninety degrees from a horizontal direction to a vertical direction by means of a cascade of turning vanes. Then, a second cascade of turning vanes turns the flow direction back to horizontal so that the flowing fluid is above the bottom branch of the circuit. A stilling section containing screens and a "honeycomb" made from sections of tubing follows the upper vanes. A contraction of the natural draw-down type (see Steele, 1962 and Preston, 1966) follows the stilling section. The test section extends from the contraction outlet to the combination weir which controls the subcritical flow in the test section by means of critical flow both over and under the weir. The fluid passing over and under the weir is directed into the sump tank beneath the test section by means of a vertical wall directly behind the weir and an inclined plate beneath the vertical wall.

This overall flume design was based on a combination of a literature survey of information about existing flumes and design methods, and an experimental study of two, 1/4 scale, model flume configurations by MacDougal (1974).

The details of the individual components of the flume will now be described in turn.

3. INDIVIDUAL FLUME COMPONENTS

Test Section. The length of the test section was dictated by the length of the space available and the portion of

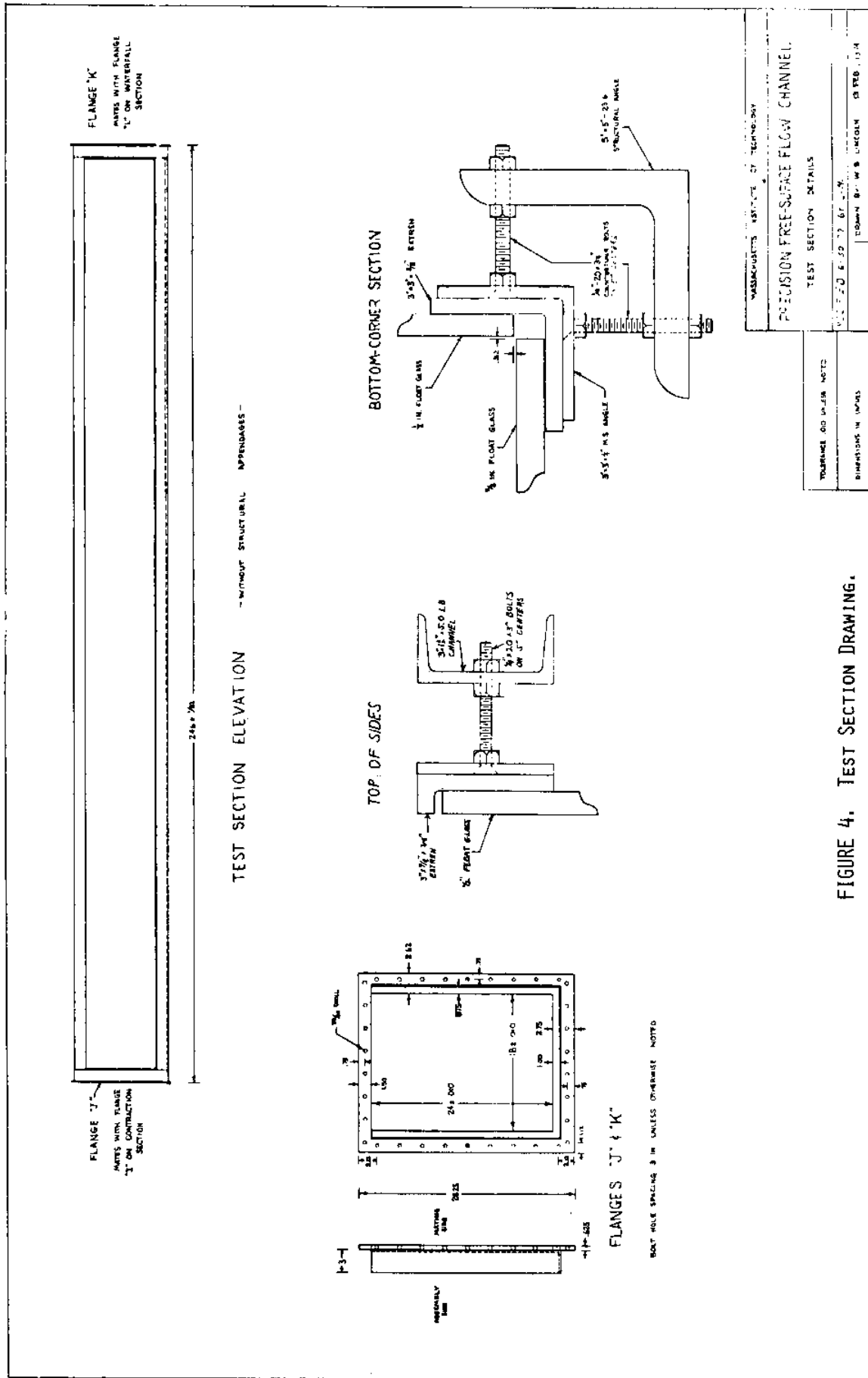


FIGURE 4. TEST SECTION DRAWING.

that length which would be taken up by the inlets and outlets to the test section. The inlet was comprised of the turning vane section, the stilling section, and the contraction. The outlet was comprised of the weir section. The resulting test section length was 20.5 feet.

The depth of the test section would ideally be determined by the desire to make the depth several times greater than the maximum depth of the oil layers to be used in the experiments. However, in light of the fact that an upstream contraction with an area ratio of about 4 was found to be needed (MacDougal, 1974), the above requirement would result in cross-sectional sizes that would be too large for our available space. As a result, the depth at the large end of the contraction was set at the maximum size compatible with the available space and funds available for flume construction which was 3 feet. This led to a test section inside width of 1.5 feet and a test section inside operating fluid depth of 1.67 feet. To provide adequate freeboard, the total test section depth was designed to be 2 feet.

Figure 4 shows a drawing of the test section. The test section sidewalls and bottom were made of glass to permit visualization and optical measurements of the experiments. In order to provide sufficient support for maintaining a tolerance of ± 0.030 inches, structural steel members were used to support the test section. As shown in Figure 4, adjusting bolts were used between the basic test section and the main supporting frames. These bolts were spaced at intervals of 5 inches.

Special consideration was necessary for the support of the lower corners and upper edges of the glass part of the test section. The main structural members were spaced a few inches away from the edges and corners as shown in Figure 4. Smaller steel structural members were affixed to the corners and edges as shown in that figure. The usual procedure for

attaching glass to steel is by means of a rubber based adhesive. This permits a small amount of motion between the glass and the steel and thereby minimizes the risk of cracking the glass due to small dimensional changes. We wished to avoid the use of the rubber based adhesive because it would have resulted in less precise dimensional control and stability than we wished to achieve. Therefore, epoxy cement was used. Although the coefficients of thermal expansion of glass and steel are similar, we felt that it was still necessary to have some material more flexible than steel between the glass and steel to allow for small dimensional changes. This was accomplished by the use of glass reinforced epoxy resin structural members (made of a material called "Extren") as shown in Figure 4. It is noted here that we have come to regret this aspect of the design as each of the two glass sidewalls later cracked (see Section 4).

Water channels which must operate between low subcritical speeds and high supercritical speeds must have an adjustable tilting test section or test section floor as described by Preston (1966). For the case of our low speed channel, we felt that a fixed setting of test section tilt could be used. However, it was not known in advance whether the test section should tilt down or tilt up for optimum operation. A test section which tilts downward in the direction of flow provides some compensation for the increase in speed of the flow outside the boundary layers with downstream position due to the thickening boundary layers on the test section walls. On the other hand, a test section which tilts upward provides an increase in flow stability and a more "wave-free" water surface. The range of tilt that either of these requirements would lead to was small enough for it to be absorbed by the rubber gaskets between various components of the flume at the upstream end of the test section so that it was only necessary for us to be able to adjust the height of the downstream end. This

was accomplished by attaching the main structural supporting members of the test section to a large vertical metal plate which forms part of the flume structure as shown in Figure 5. Initially, we planned to bolt brackets on the test section supporting members to the plate. However, assembly difficulties led us to weld the brackets to the plate with the intent of cutting the welds free and rewelding if a change in test section tilt was found desirable. Our initial installation was made with the downstream end of the test section $1/8$ inch lower than the upstream end.

Overall Flume Structural Support. The M.I.T. oil layer flume was built on the second floor of a building. This building has a floor supported by steel beams located on 15-foot centers and fastened to columns in the building walls. The flume spans three beams. The overall weight of the water-filled flume was estimated to be 30,000 pounds and it was felt that with much of this load on the concrete floor between beams the safety factor for the floor was insufficient. The floor beams themselves and the columns to which they were attached were found to be more than adequately strong. In order to distribute the flume weight over the floor beams without excessive floor loading it was concluded that an overall steel supporting structure would be best. An isometric drawing of this structure is shown in Figure 5. The basic longitudinal support of the flume is supplied by 8 inch by 8 inch by $1/2$ inch thick I-beams. The basic geometry of the flume was best achieved by having the bottom of the sump tank a nominal distance of 11 inches above the floor so that $1-1/2$ inch by 3 inch by $1/4$ inch thick channels with the $1-1/2$ inch face horizontal were welded to the tops of the I-beams. An epoxy-base grouting mixture was used between the beams and the floor inasmuch as up to 1 inch of floor sag existed between floor beams. Steel studs were driven into the concrete floor on 4-foot centers with these studs

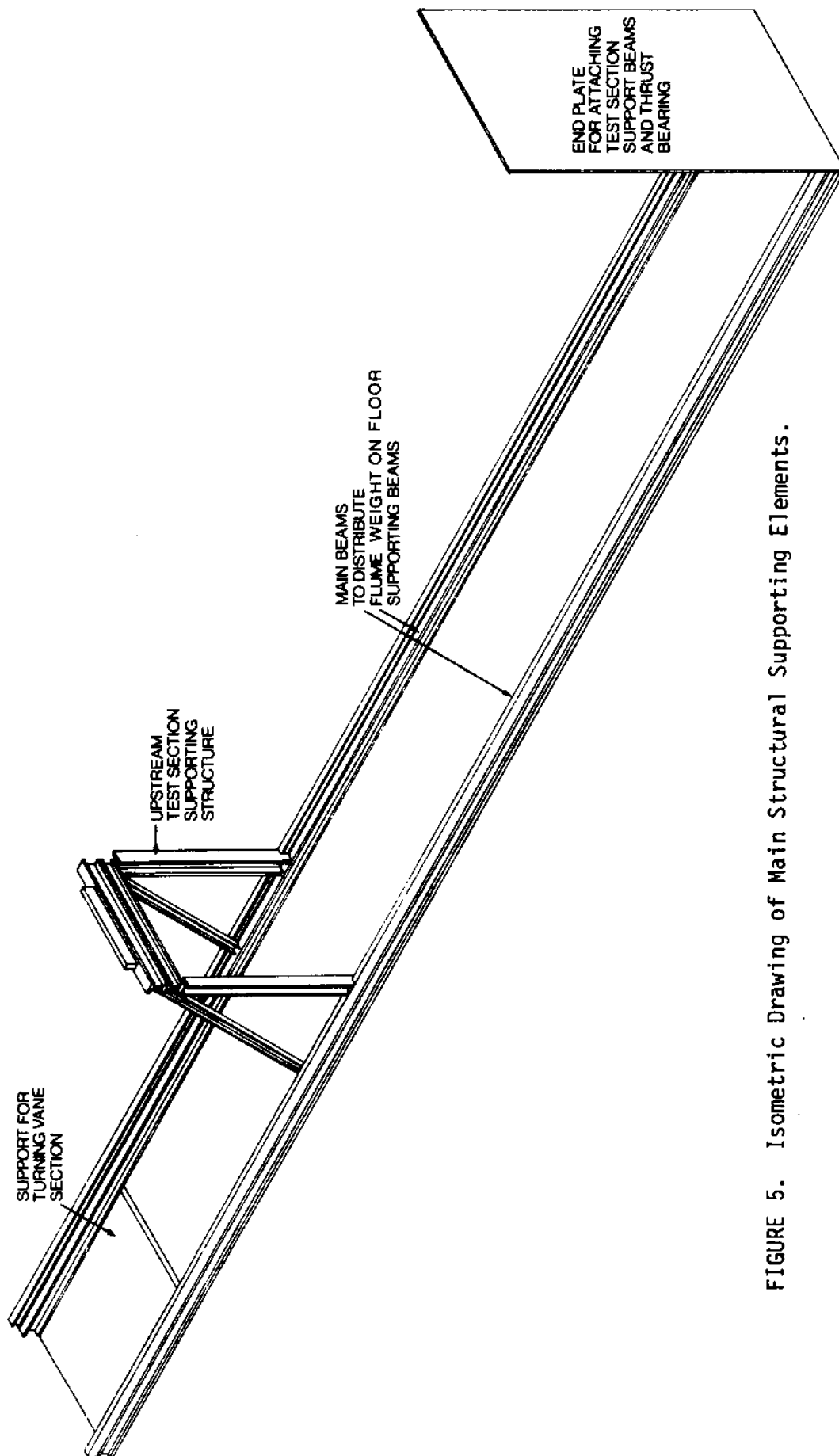


FIGURE 5. Isometric Drawing of Main Structural Supporting Elements.

passing through the I-beam flanges and with the flanges secured to the threaded studs by nuts.

At one end of the flume, where the turning vane section would be located, a 1 inch thick steel plate was welded between the I-beam webs just above the lower flanges. The space between the floor and the bottom of this plate was filled with concrete. At the downstream end of the flume, a tall vertical steel plate, 1/2 inch thick, was welded to the ends of the I-beams. The main test section supporting structure was ultimately attached to this steel plate.

Following the construction of the flume, we felt that the test section deflection might be excessive so that vertical steel rods were run between the test section and two ceiling beams which supported the floor above (see Figure 3). These rods were fitted with turnbuckles in order to be able to obtain precise length adjustments.

Weir Section. For subcritical flumes, the studies of Steele (1962) indicated that either a tilting weir or a cascade weir would be satisfactory for the exit of the test section. A tilting weir is simply a vertical plate hinged at its bottom with the fluid passing over its top and the fluid then falling into a sump. The flow over the top of the weir is locally at critical speed and as a result, the height of the weir controls the fluid flow in the test section. For example, with the use of a tilting weir; to raise the flow speed from one condition to another while maintaining a fixed test section fluid depth, the weir would be rotated about its hinge at the bottom of the test section so as to lower the top of the weir and the flume pump speed would be simultaneously increased so that the initial test section fluid depth would be retained with an increased depth of critical flow over the top of the weir.

A cascade weir is a cascade of airfoils whose spans are horizontal and which extend across the test section. By simultaneously adjusting the pitch angle of all the airfoils (much like the operation of a venetian blind) the height of the slots between the airfoils is changed. The flow rate through the test section is controlled by adjusting the airfoil pitch angles.

Inasmuch as the tilting type weir was easier and less expensive to construct, we decided to initially build a modified form of the tilting weir; with the design being of the type that would allow changing to another type of weir if that was found to be required. The modified tilting weir we built has its hinge above the channel bottom so that flow leaves the test section both over the weir and under the weir thus making the device a combination between a sharp crested weir and a sluice gate. Figures 2 and 3 show the weir section as it is located in the flume. Figure 6 is a sketch of the geometry of the tilting combination weir. The location of the axis of rotation of the weir was chosen such that the total flow rate under the weir and the total flow rate over the weir were roughly equal over the anticipated range of operating flume speeds for a fluid depth in the flume test section of 1.67 feet. The approximate flow rates are calculated as follows. The flow over the weir in ft^3/sec is given approximately by Nelson (1976) as:

$$Q_1 = 3.3WH^{3/2} \quad (1)$$

where W is the width of the channel in feet and H is the height of the upstream surface above the top edge of the weir in feet. Similarly, Nelson (1976) indicates that the depth of the vena contracta behind a sluice gate is approximately 0.75 times the height of the opening in the gate. This leads to an equation

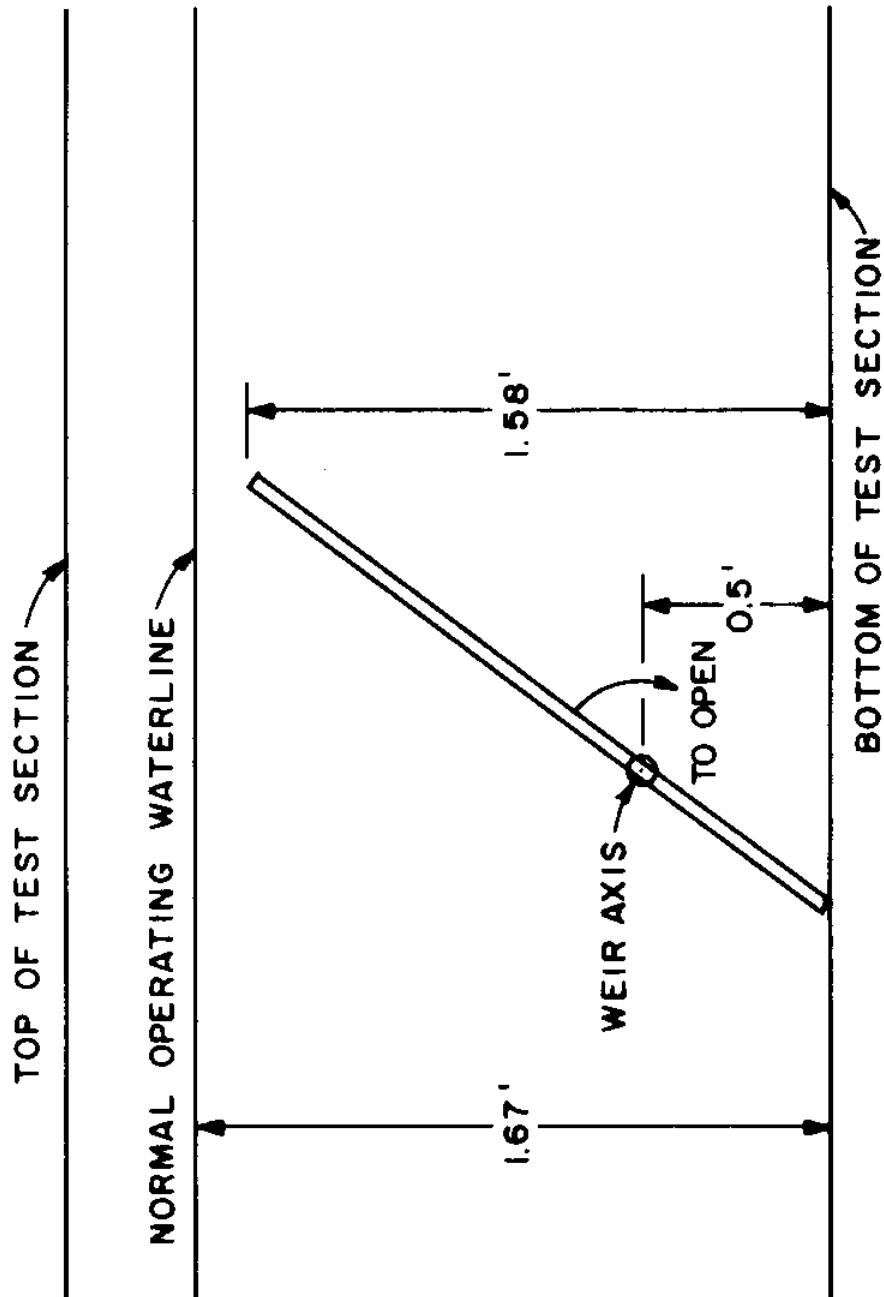


FIGURE 6. Geometry of Tilting Weir Section.
The tilting weir is used to control the flow at the downstream end of the test section.

for the approximate flow rate beneath the gate of

$$Q_2 = 6.02Wh\sqrt{d} \quad (2)$$

where h is the height of the opening between the channel bottom and the gate and d is the depth of the center of the gate opening below the free surface in the test section.

We found that Q_1 and Q_2 would be roughly equal if the weir axis was located 0.5 feet above the channel bottom with the weir length chosen so its top was 1.58 feet above the bottom when the bottom opening was fully closed. This is the arrangement shown in Figure 6. For this arrangement,

$$H = 2.13h + .08 \quad (3)$$

Table 1 shows the flow rates and flume test section velocity for various weir positions. The test section velocity (in ft/sec) is given by

$$V = \frac{Q_1 + Q_2}{2.51} \quad (4)$$

Figure 7 shows graphs of the flow rates over and under the weir for various values of the height of the opening under the weir with the above-weir height given by Equation (3).

In operation, it was found that there was considerable splashing of the water that came over or under the weir and it was difficult to prevent some of this splashing from going between the steel structural plate and the downstream end of the sump tank. This problem was overcome by installation of the tilted board beneath the weir section as shown in Figures 2 and 3. This board serves as a deflector of the flow from the weir section into the sump tank.

TABLE 1.

Weir Flows and Test Sections Flow Speeds
for Various Weir Setting

h	.	H	.	Q_1	.	Q_2	.	V
Opening Below Weir (ft)	.	Upstream Water Surface Height Above Weir (ft)	.	Flow Rate Above Weir (ft ³ /sec)	.	Flow Rate Below Weir (ft ³ /sec)	.	Mean Test Section Speed (ft/sec)
0.00	.	0.08	.	0.112	.	0.000	.	0.045
0.10	.	0.29	.	0.773	.	1.106	.	0.749
0.20	.	0.51	.	1.803	.	2.212	.	1.600
0.30	.	0.72	.	3.024	.	3.318	.	2.527
0.40	.	0.93	.	4.439	.	4.424	.	3.531
0.45	.	1.04	.	5.250	.	4.980	.	4.070

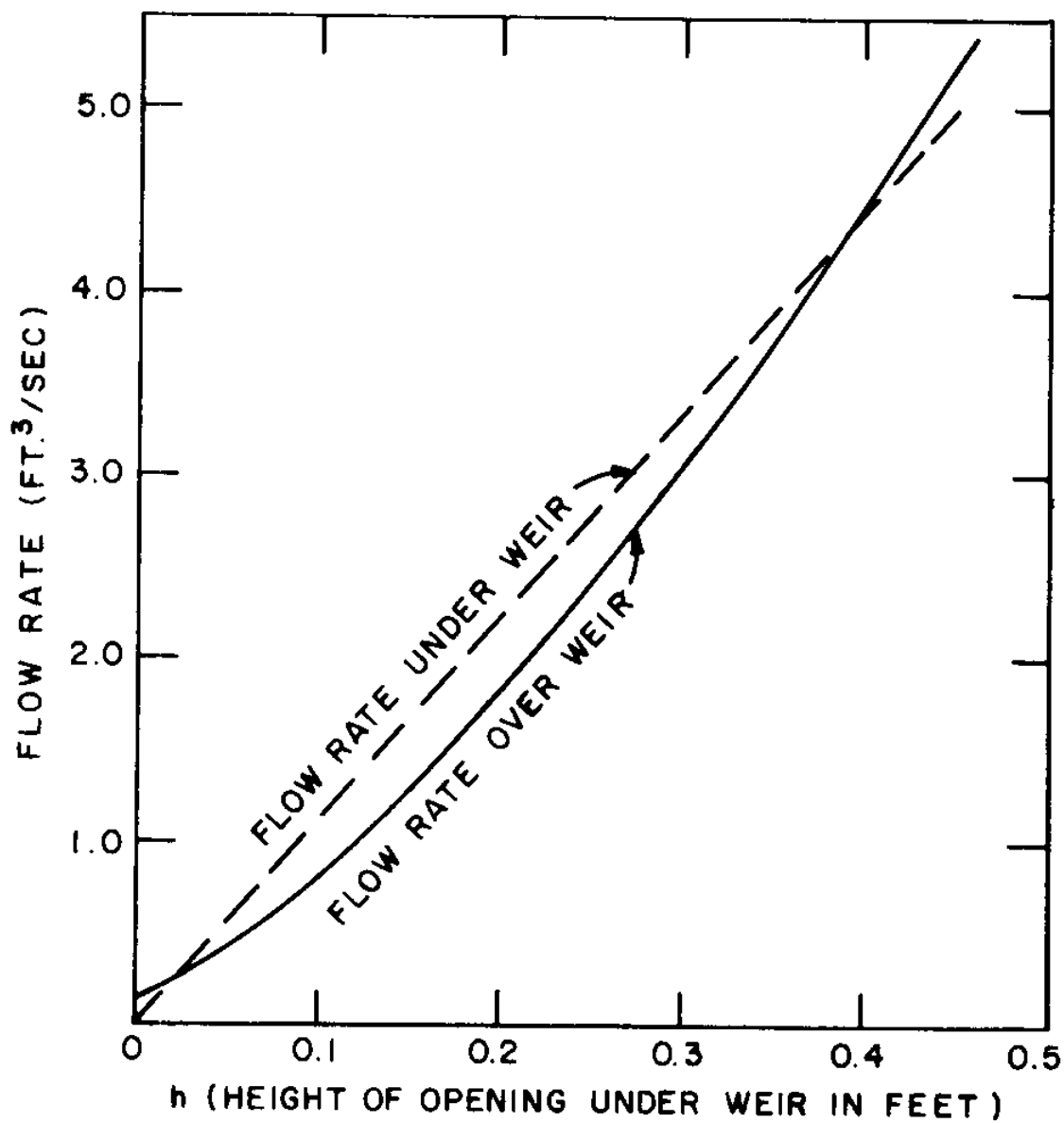


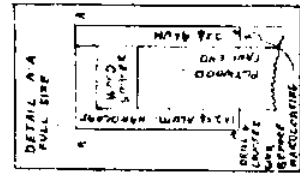
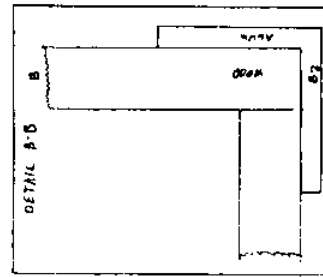
FIGURE 7. Weir Flows versus Opening Beneath Weir.
This figure is based on the geometry shown
in Figure 6.

Sump Tank. The purposes of the sump tank are to remove entrained air from the water, to provide an inlet to the flume impeller, and to provide a space for oil to collect during and after flume experiments with provision for removing this oil from the surface of the fluid in the sump tank. A basic requirement on sump tank geometry is that it should be as large as space limitations will permit. Larger size leads to more time available for the removal of entrained air. The tendency of the impeller to draw in air is diminished by increasing the fluid depth in the sump tank above the impeller nozzle inlet. Acceptable sump tank performance was achieved with a tank that is 16 feet long, 4 feet wide and 4 feet high. The sump tank is shown in the flume drawings of Figures 2 and 3. A construction drawing of the sump tank is shown in Figure 8.

The sump tank has a screen across its entire cross section at a distance of 7.5 feet from the downstream end (end nearest impeller) of the tank. This screen removes some air bubbles from the stream and eliminates any especially high velocities in the axial flow to prevent parcels of fluid containing entrained air from getting to the sump tank outlet before the air has a chance to rise. The sump tank width is 4 feet and the normal fluid depth is 3.28 feet giving a sump tank operating cross-sectional area of 13.12 square feet of fluid. Therefore, for test section operating velocities of 0 to 4 ft/sec, the mean axial velocity in the sump tank lies in the range of 0 to .77 ft/sec. As a result, the mean transit time of fluid from the screen to the sump tank outlet is always more than 9.7 seconds.

The sump tank outlet occupies the lower 1.67 feet of height at the downstream end of the tank. This gives an inlet area to the impeller nozzle of 6.68 square feet, which results in a range of nozzle inlet speeds from 0 to 1.5 ft/sec. The dynamic head associated with the nozzle inlet flow speed lies between 0 and 0.4 feet and this is small enough for the entrainment of air

- LIST OF MATERIALS**
- 8 SHEETS 1/2" x 12" MARINE PLYWOOD - SHERITT
 - 80' 3" x 1/2" x 1/2" ROUGH BATTENED ALUM. ANGLE ONE-PASS
 - 60' 3" x 1/2" x 1/2" ROUGH BATTENED ALUM. ANGLE ONE-PASS
 - 4' 3" x 1/2" x 1/2" ROUGH BATTENED ALUM. ANGLE ONE-PASS
 - 4' 3" x 1/2" x 1/2" ROUGH BATTENED ALUM. ANGLE ONE-PASS
 - 120' 1/2" x 1/2" x 1/2" ROUGH BATTENED ALUM. ANGLE ONE-PASS
 - 8' 1/2" x 1/2" x 1/2" ROUGH BATTENED ALUM. ANGLE ONE-PASS
 - 80' 1/2" x 1/2" x 1/2" ROUGH BATTENED ALUM. ANGLE ONE-PASS
 - 80' 1/2" x 1/2" x 1/2" ROUGH BATTENED ALUM. ANGLE ONE-PASS
 - 8 GALLONS EPOXY PUTTY - HARDENER R-2
 - 8 GALLONS EPOXY PUTTY - HARDENER R-2
 - 3 GALLONS INTER - PAINT



SUMP TANK

CROSS BEAMS UNDER BASE AT LOCATIONS QY, Z, O;
 4' 6" 9" 12" 15" 18" 21" 24" 27" 30" 33" 36" 39" 42" 45" 48" 51" 54" 57" 60" 63" 66" 69" 72" 75" 78" 81" 84" 87" 90" 93" 96" 99" 102" 105" 108" 111" 114" 117" 120" 123" 126" 129" 132" 135" 138" 141" 144" 147" 150" 153" 156" 159" 162" 165" 168" 171" 174" 177" 180" 183" 186" 189" 192" 195" 198" 201" 204" 207" 210" 213" 216" 219" 222" 225" 228" 231" 234" 237" 240" 243" 246" 249" 252" 255" 258" 261" 264" 267" 270" 273" 276" 279" 282" 285" 288" 291" 294" 297" 300" 303" 306" 309" 312" 315" 318" 321" 324" 327" 330" 333" 336" 339" 342" 345" 348" 351" 354" 357" 360" 363" 366" 369" 372" 375" 378" 381" 384" 387" 390" 393" 396" 399" 402" 405" 408" 411" 414" 417" 420" 423" 426" 429" 432" 435" 438" 441" 444" 447" 450" 453" 456" 459" 462" 465" 468" 471" 474" 477" 480" 483" 486" 489" 492" 495" 498" 501" 504" 507" 510" 513" 516" 519" 522" 525" 528" 531" 534" 537" 540" 543" 546" 549" 552" 555" 558" 561" 564" 567" 570" 573" 576" 579" 582" 585" 588" 591" 594" 597" 600" 603" 606" 609" 612" 615" 618" 621" 624" 627" 630" 633" 636" 639" 642" 645" 648" 651" 654" 657" 660" 663" 666" 669" 672" 675" 678" 681" 684" 687" 690" 693" 696" 699" 702" 705" 708" 711" 714" 717" 720" 723" 726" 729" 732" 735" 738" 741" 744" 747" 750" 753" 756" 759" 762" 765" 768" 771" 774" 777" 780" 783" 786" 789" 792" 795" 798" 801" 804" 807" 810" 813" 816" 819" 822" 825" 828" 831" 834" 837" 840" 843" 846" 849" 852" 855" 858" 861" 864" 867" 870" 873" 876" 879" 882" 885" 888" 891" 894" 897" 900" 903" 906" 909" 912" 915" 918" 921" 924" 927" 930" 933" 936" 939" 942" 945" 948" 951" 954" 957" 960" 963" 966" 969" 972" 975" 978" 981" 984" 987" 990" 993" 996" 999" 1002" 1005" 1008" 1011" 1014" 1017" 1020" 1023" 1026" 1029" 1032" 1035" 1038" 1041" 1044" 1047" 1050" 1053" 1056" 1059" 1062" 1065" 1068" 1071" 1074" 1077" 1080" 1083" 1086" 1089" 1092" 1095" 1098" 1101" 1104" 1107" 1110" 1113" 1116" 1119" 1122" 1125" 1128" 1131" 1134" 1137" 1140" 1143" 1146" 1149" 1152" 1155" 1158" 1161" 1164" 1167" 1170" 1173" 1176" 1179" 1182" 1185" 1188" 1191" 1194" 1197" 1200" 1203" 1206" 1209" 1212" 1215" 1218" 1221" 1224" 1227" 1230" 1233" 1236" 1239" 1242" 1245" 1248" 1251" 1254" 1257" 1260" 1263" 1266" 1269" 1272" 1275" 1278" 1281" 1284" 1287" 1290" 1293" 1296" 1299" 1302" 1305" 1308" 1311" 1314" 1317" 1320" 1323" 1326" 1329" 1332" 1335" 1338" 1341" 1344" 1347" 1350" 1353" 1356" 1359" 1362" 1365" 1368" 1371" 1374" 1377" 1380" 1383" 1386" 1389" 1392" 1395" 1398" 1401" 1404" 1407" 1410" 1413" 1416" 1419" 1422" 1425" 1428" 1431" 1434" 1437" 1440" 1443" 1446" 1449" 1452" 1455" 1458" 1461" 1464" 1467" 1470" 1473" 1476" 1479" 1482" 1485" 1488" 1491" 1494" 1497" 1500" 1503" 1506" 1509" 1512" 1515" 1518" 1521" 1524" 1527" 1530" 1533" 1536" 1539" 1542" 1545" 1548" 1551" 1554" 1557" 1560" 1563" 1566" 1569" 1572" 1575" 1578" 1581" 1584" 1587" 1590" 1593" 1596" 1599" 1602" 1605" 1608" 1611" 1614" 1617" 1620" 1623" 1626" 1629" 1632" 1635" 1638" 1641" 1644" 1647" 1650" 1653" 1656" 1659" 1662" 1665" 1668" 1671" 1674" 1677" 1680" 1683" 1686" 1689" 1692" 1695" 1698" 1701" 1704" 1707" 1710" 1713" 1716" 1719" 1722" 1725" 1728" 1731" 1734" 1737" 1740" 1743" 1746" 1749" 1752" 1755" 1758" 1761" 1764" 1767" 1770" 1773" 1776" 1779" 1782" 1785" 1788" 1791" 1794" 1797" 1800" 1803" 1806" 1809" 1812" 1815" 1818" 1821" 1824" 1827" 1830" 1833" 1836" 1839" 1842" 1845" 1848" 1851" 1854" 1857" 1860" 1863" 1866" 1869" 1872" 1875" 1878" 1881" 1884" 1887" 1890" 1893" 1896" 1899" 1902" 1905" 1908" 1911" 1914" 1917" 1920" 1923" 1926" 1929" 1932" 1935" 1938" 1941" 1944" 1947" 1950" 1953" 1956" 1959" 1962" 1965" 1968" 1971" 1974" 1977" 1980" 1983" 1986" 1989" 1992" 1995" 1998" 2001" 2004" 2007" 2010" 2013" 2016" 2019" 2022" 2025" 2028" 2031" 2034" 2037" 2040" 2043" 2046" 2049" 2052" 2055" 2058" 2061" 2064" 2067" 2070" 2073" 2076" 2079" 2082" 2085" 2088" 2091" 2094" 2097" 2100" 2103" 2106" 2109" 2112" 2115" 2118" 2121" 2124" 2127" 2130" 2133" 2136" 2139" 2142" 2145" 2148" 2151" 2154" 2157" 2160" 2163" 2166" 2169" 2172" 2175" 2178" 2181" 2184" 2187" 2190" 2193" 2196" 2199" 2202" 2205" 2208" 2211" 2214" 2217" 2220" 2223" 2226" 2229" 2232" 2235" 2238" 2241" 2244" 2247" 2250" 2253" 2256" 2259" 2262" 2265" 2268" 2271" 2274" 2277" 2280" 2283" 2286" 2289" 2292" 2295" 2298" 2301" 2304" 2307" 2310" 2313" 2316" 2319" 2322" 2325" 2328" 2331" 2334" 2337" 2340" 2343" 2346" 2349" 2352" 2355" 2358" 2361" 2364" 2367" 2370" 2373" 2376" 2379" 2382" 2385" 2388" 2391" 2394" 2397" 2400" 2403" 2406" 2409" 2412" 2415" 2418" 2421" 2424" 2427" 2430" 2433" 2436" 2439" 2442" 2445" 2448" 2451" 2454" 2457" 2460" 2463" 2466" 2469" 2472" 2475" 2478" 2481" 2484" 2487" 2490" 2493" 2496" 2499" 2502" 2505" 2508" 2511" 2514" 2517" 2520" 2523" 2526" 2529" 2532" 2535" 2538" 2541" 2544" 2547" 2550" 2553" 2556" 2559" 2562" 2565" 2568" 2571" 2574" 2577" 2580" 2583" 2586" 2589" 2592" 2595" 2598" 2601" 2604" 2607" 2610" 2613" 2616" 2619" 2622" 2625" 2628" 2631" 2634" 2637" 2640" 2643" 2646" 2649" 2652" 2655" 2658" 2661" 2664" 2667" 2670" 2673" 2676" 2679" 2682" 2685" 2688" 2691" 2694" 2697" 2700" 2703" 2706" 2709" 2712" 2715" 2718" 2721" 2724" 2727" 2730" 2733" 2736" 2739" 2742" 2745" 2748" 2751" 2754" 2757" 2760" 2763" 2766" 2769" 2772" 2775" 2778" 2781" 2784" 2787" 2790" 2793" 2796" 2799" 2802" 2805" 2808" 2811" 2814" 2817" 2820" 2823" 2826" 2829" 2832" 2835" 2838" 2841" 2844" 2847" 2850" 2853" 2856" 2859" 2862" 2865" 2868" 2871" 2874" 2877" 2880" 2883" 2886" 2889" 2892" 2895" 2898" 2901" 2904" 2907" 2910" 2913" 2916" 2919" 2922" 2925" 2928" 2931" 2934" 2937" 2940" 2943" 2946" 2949" 2952" 2955" 2958" 2961" 2964" 2967" 2970" 2973" 2976" 2979" 2982" 2985" 2988" 2991" 2994" 2997" 3000" 3003" 3006" 3009" 3012" 3015" 3018" 3021" 3024" 3027" 3030" 3033" 3036" 3039" 3042" 3045" 3048" 3051" 3054" 3057" 3060" 3063" 3066" 3069" 3072" 3075" 3078" 3081" 3084" 3087" 3090" 3093" 3096" 3099" 3102" 3105" 3108" 3111" 3114" 3117" 3120" 3123" 3126" 3129" 3132" 3135" 3138" 3141" 3144" 3147" 3150" 3153" 3156" 3159" 3162" 3165" 3168" 3171" 3174" 3177" 3180" 3183" 3186" 3189" 3192" 3195" 3198" 3201" 3204" 3207" 3210" 3213" 3216" 3219" 3222" 3225" 3228" 3231" 3234" 3237" 3240" 3243" 3246" 3249" 3252" 3255" 3258" 3261" 3264" 3267" 3270" 3273" 3276" 3279" 3282" 3285" 3288" 3291" 3294" 3297" 3300" 3303" 3306" 3309" 3312" 3315" 3318" 3321" 3324" 3327" 3330" 3333" 3336" 3339" 3342" 3345" 3348" 3351" 3354" 3357" 3360" 3363" 3366" 3369" 3372" 3375" 3378" 3381" 3384" 3387" 3390" 3393" 3396" 3399" 3402" 3405" 3408" 3411" 3414" 3417" 3420" 3423" 3426" 3429" 3432" 3435" 3438" 3441" 3444" 3447" 3450" 3453" 3456" 3459" 3462" 3465" 3468" 3471" 3474" 3477" 3480" 3483" 3486" 3489" 3492" 3495" 3498" 3501" 3504" 3507" 3510" 3513" 3516" 3519" 3522" 3525" 3528" 3531" 3534" 3537" 3540" 3543" 3546" 3549" 3552" 3555" 3558" 3561" 3564" 3567" 3570" 3573" 3576" 3579" 3582" 3585" 3588" 3591" 3594" 3597" 3600" 3603" 3606" 3609" 3612" 3615" 3618" 3621" 3624" 3627" 3630" 3633" 3636" 3639" 3642" 3645" 3648" 3651" 3654" 3657" 3660" 3663" 3666" 3669" 3672" 3675" 3678" 3681" 3684" 3687" 3690" 3693" 3696" 3699" 3702" 3705" 3708" 3711" 3714" 3717" 3720" 3723" 3726" 3729" 3732" 3735" 3738" 3741" 3744" 3747" 3750" 3753" 3756" 3759" 3762" 3765" 3768" 3771" 3774" 3777" 3780" 3783" 3786" 3789" 3792" 3795" 3798" 3801" 3804" 3807" 3810" 3813" 3816" 3819" 3822" 3825" 3828" 3831" 3834" 3837" 3840" 3843" 3846" 3849" 3852" 3855" 3858" 3861" 3864" 3867" 3870" 3873" 3876" 3879" 3882" 3885" 3888" 3891" 3894" 3897" 3900" 3903" 3906" 3909" 3912" 3915" 3918" 3921" 3924" 3927" 3930" 3933" 3936" 3939" 3942" 3945" 3948" 3951" 3954" 3957" 3960" 3963" 3966" 3969" 3972" 3975" 3978" 3981" 3984" 3987" 3990" 3993" 3996" 3999" 4002" 4005" 4008" 4011" 4014" 4017" 4020" 4023" 4026" 4029" 4032" 4035" 4038" 4041" 4044" 4047" 4050" 4053" 4056" 4059" 4062" 4065" 4068" 4071" 4074" 4077" 4080" 4083" 4086" 4089" 4092" 4095" 4098" 4101" 4104" 4107" 4110" 4113" 4116" 4119" 4122" 4125" 4128" 4131" 4134" 4137" 4140" 4143" 4146" 4149" 4152" 4155" 4158" 4161" 4164" 4167" 4170" 4173" 4176" 4179" 4182" 4185" 4188" 4191" 4194" 4197" 4200" 4203" 4206" 4209" 4212" 4215" 4218" 4221" 4224" 4227" 4230" 4233" 4236" 4239" 4242" 4245" 4248" 4251" 4254" 4257" 4260" 4263" 4266" 4269" 4272" 4275" 4278" 4281" 4284" 4287" 4290" 4293" 4296" 4299" 4302" 4305" 4308" 4311" 4314" 4317" 4320" 4323" 4326" 4329" 4332" 4335" 4338" 4341" 4344" 4347" 4350" 4353" 4356" 4359" 4362" 4365" 4368" 4371" 4374" 4377" 4380" 4383" 4386" 4389" 4392" 4395" 4398" 4401" 4404" 4407" 4410" 4413" 4416" 4419" 4422" 4425" 4428" 4431" 4434" 4437" 4440" 4443" 4446" 4449" 4452" 4455" 4458" 4461" 4464" 4467" 4470" 4473" 4476" 4479" 4482" 4485" 4488" 4491" 4494" 4497" 4500" 4503" 4506" 4509" 4512" 4515" 4518" 4521" 4524" 4527" 4530" 4533" 4536" 4539" 4542" 4545" 4548" 4551" 4554" 4557" 4560" 4563" 4566" 4569" 4572" 4575" 4578" 4581" 4584" 4587" 4590" 4593" 4596" 4599" 4602" 4605" 4608" 4611" 4614" 4617" 4620" 4623" 4626" 4629" 4632" 4635" 4638" 4641" 4644" 4647" 4650" 4653" 4656" 4659" 4662" 4665" 4668" 4671" 4674" 4677" 4680" 4683" 4686" 4689" 4692" 4695" 4698" 4701" 4704" 4707" 4710" 4713" 4716" 4719" 4722" 4725" 4728" 4731" 4734" 4737" 4740" 4743" 4746" 4749" 4752" 4755" 4758" 4761" 4764" 4767" 4770" 4773" 4776" 4779" 4782" 4785" 4788" 4791" 4794" 4797" 4800" 4803" 4806" 4809" 4812" 4815" 4818" 4821" 4824" 4827" 4830" 4833" 4836" 4839" 4842" 4845" 4848" 4851" 4854" 4857" 4860" 4863" 4866" 4869" 4872" 4875" 4878" 4881" 4884" 4887" 4890" 4893" 4896" 4899" 4902" 4905" 4908" 4911" 4914" 4917" 4920" 4923" 4926" 4929" 4932" 4935" 4938" 4941" 4944" 4947" 4950" 4953" 4956" 4959" 4962" 4965" 4968" 4971" 4974" 4977" 4980" 4983" 4986" 4989" 4992" 4995" 4998" 5001" 5004" 5007" 5010" 5013" 5016" 5019" 5022" 5025" 5028" 5031" 5034" 5037" 5040" 5043" 5046" 5049" 5052" 5055" 5058" 5061" 5064" 5067" 5070" 5073" 5076" 5079" 5082" 5085" 5088" 5091" 5094" 5097" 5100" 5103" 5106" 5109" 5112" 5115" 5118" 5121" 5124" 5127" 5130" 5133" 5136" 5139" 5142" 5145" 5148" 5151" 5154" 5157" 5160" 5163" 5166" 5169" 5172" 5175" 5178" 5181" 5184" 5187" 5190" 5193" 5196" 5199" 5202" 5205" 5208" 5211" 5214" 5217" 5220" 5223" 5226" 5229" 5232" 5235" 5238" 5241" 5244" 5247" 5250" 5253" 5256" 5259" 5262" 5265" 5268" 5271" 5274" 5277" 5280" 5283" 5286" 5289" 5292" 5295" 5298" 5301" 5304" 5307" 5310" 5313" 5316" 5319" 5322" 5325" 5328" 5331" 5334" 5337" 5340" 5343" 5346" 5349" 5352" 5355" 5358" 5361" 5364" 5367" 5370" 5373" 5376" 5379" 5382" 5385" 5388" 5391" 5394" 5397" 5400" 5403" 5406" 5409" 5412" 5415" 5418" 5421" 5424" 5427" 5430" 5433" 5436" 5439" 5442" 5445" 5448" 5451" 5454" 5457" 5460" 5463" 5466" 5469" 5472" 5475" 5478" 5481" 5484" 5487" 5490" 5493" 5496" 5499" 5502" 5505" 5508" 5511" 5514" 5517" 5520" 5523" 5526" 5529" 5532" 5535" 5538" 5541" 5544" 5547" 5550" 5553" 5556" 5559" 5562" 5565" 5568" 5571" 5574" 5577" 5580" 5583" 5586" 5589" 5592" 5595" 5598" 5601" 5604" 5607" 5610" 5613" 5616" 5619" 5622" 5625" 5628" 5631" 5634" 5637" 5640" 5643" 5646" 5649" 5652" 5655" 5658" 5661" 5664" 5667" 5670" 5673" 5676" 5679" 5682" 5685" 5688" 5691" 5694" 5697" 5700" 5703" 5706" 5709" 5712" 5715" 5718" 5721" 5724" 5727" 5730" 5733" 5736" 5739" 5742" 5745" 5748" 5751" 5754" 5757" 5760" 5763" 5766" 5769" 5772" 5775" 5778" 5781" 5784" 5787" 5790" 5793" 5796" 5799" 5802" 5805" 5808" 5811" 5814" 5817" 5820" 5823" 5826" 5829" 5832" 5835" 5838" 5841" 5844" 5847" 5850" 5853" 5856" 5859" 5862" 5865" 5868" 5871" 5874" 5877" 5880" 5883" 5886" 5889" 5892" 5895" 5898" 5901" 5904" 5907" 5910" 5913" 5916" 5919" 5922" 5925" 5928" 5931" 5934" 5937" 5940" 5943" 5946" 5949" 5952" 5955" 5958" 5961" 5964" 5967" 5970" 5973" 5976" 5979" 5982" 5985" 5988" 5991" 5994" 5997" 6000" 6003" 6006" 6009" 60

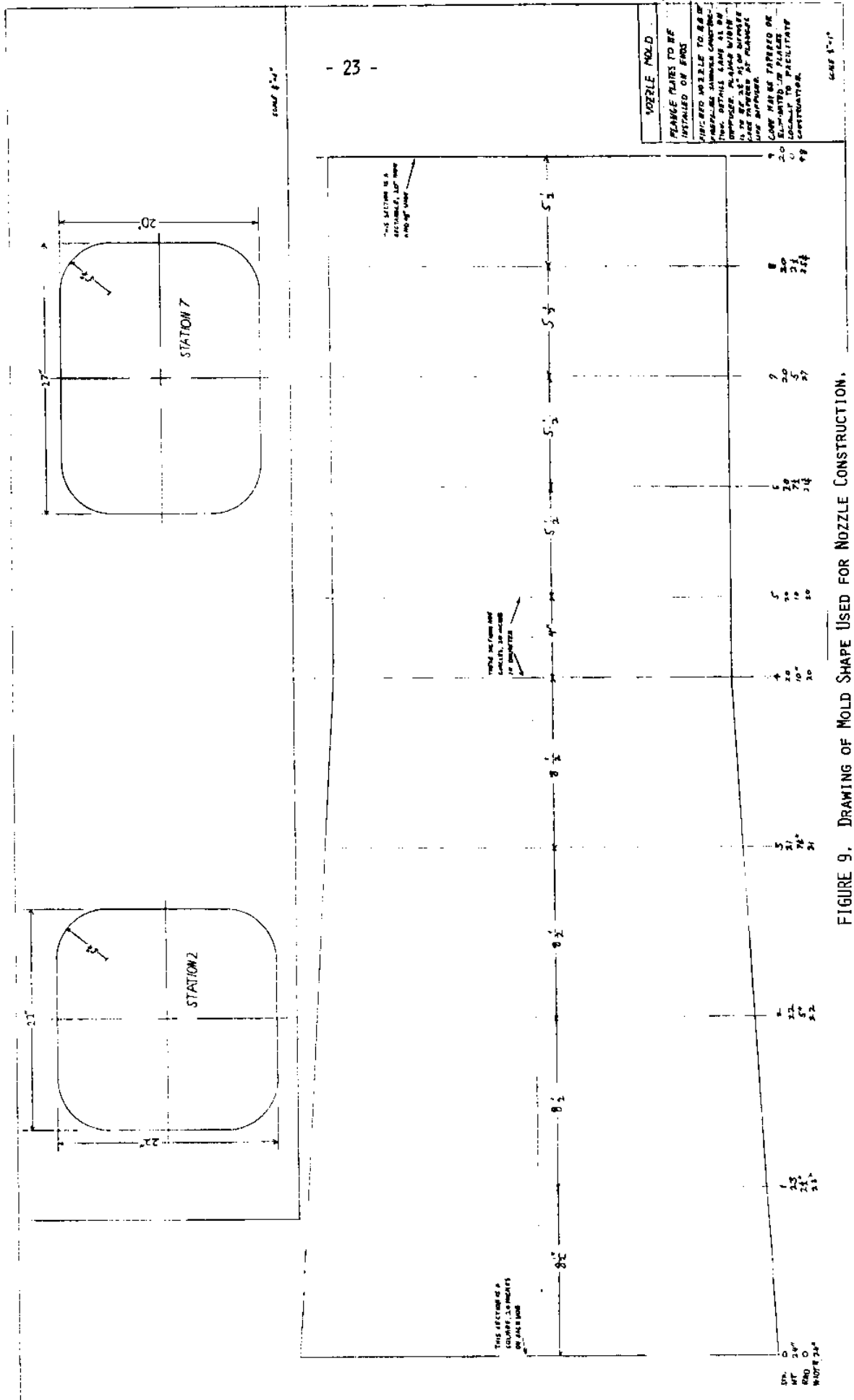
that is above the impeller nozzle inlet into the impeller to be negligible. A screen covers the impeller nozzle inlet section in order to make the velocity of the fluid leaving the sump tank and entering the impeller nozzle as uniform as possible and to prevent any objects that fall into the tank from being drawn into the impeller.

Although the top of one of the long sides of the sump tank is 4 feet above the tank bottom, a 10 foot long section of one long side is lowered to a height of 3.28 feet above the bottom. This provides a weir between the sump tank and an auxiliary tank shown in Figure 3. When the flume is started up, fluid from the sump tank fills the upper branch of the flume and the level of fluid in the sump tank goes down. This fluid is replaced by pumping water from the auxiliary tank back into the sump tank until the water level reaches the height of the weir 3.28 feet above the bottom. When the flume is shut off, the water level in the sump tank rises and spills over the weir into the auxiliary tank. The auxiliary tank is 12 feet long, 4 feet high, and 3.2 feet wide. When the flume is not operating, the water level in both the sump tank and the auxiliary tank is approximately 3.7 feet above the bottoms of the tanks so that the free surface is continuous across both the sump tank and the auxiliary tank.

For removing oil from the sump and auxiliary tanks, the downstream ends of both tanks are fitted with skimming weirs as shown in Figures 2 and 3. Oil is driven from the upstream end (end closest to the tilting weir section) of the sump tank toward the skimming weirs by surface currents induced by air bubble streams coming from perforated pipes on the bottoms of both tanks as shown in Figures 2 and 3. The air pipes have one hole of 0.050-inch diameter every 4 inches. By driving the oil toward the weirs and controlling the water height in the sump tanks by means of water feed, the oil is removed by the skimming weirs.

Nozzle Section, Impeller, Shaft and Motor. The nozzle section on the lower branch of the flume begins at the sump tank outlet and extends over a length of 5 feet. At the nozzle inlet, the cross section is a rectangle 1.67 feet high by 4 feet wide. The centerplane of the impeller is 2 feet from the upstream end (nearest sump tank) of the nozzle section. At the impeller centerplane, the nozzle cross-sectional shape is a circle with a diameter of 1.67 feet. From the nozzle inlet to the impeller centerplane, the nozzle cross section undergoes a smooth transition. The downstream end of the nozzle has a cross section which is a square 2 feet by 2 feet. This is 3 feet downstream from the centerplane of the impeller. The cross-sectional shape from the propeller to the downstream end also undergoes a smooth transition. The nozzle section is made of fiberglass that was laid up over a male mold, with the mold broken out of the nozzle after the lay up was completed. A drawing of the nozzle is shown in Figure 9.

The major power usage of this flume is the lifting of the water from the sump tank to the test section. Overcoming the static head of 2.5 feet requires 2.84 horsepower for a test section flow speed of 4 ft/sec. The potential energy imparted to the water in this lifting is lost when the water falls over or under the weir into the sump tank. The power required to achieve one dynamic head at a test section speed of 4 ft/sec is 0.28 horsepower. Since the dynamic head is so small in comparison to the static head, the dynamic head losses only need to be estimated approximately in determining flume power requirements. One dynamic head is lost as the fluid goes from the test section into the sump tank over the weir. The flume contains several screens and two sets of turning vanes, but at these devices the cross section is relatively large so the flow speed is small. Certainly, the dynamic power loss does not exceed 1.5 horsepower,



so that the total fluid power does not exceed 4.34 horsepower. Since an impeller efficiency of 0.6 is the least that would be expected, 7.5 horsepower would be sufficient to drive the flume. However, to be conservative, a 10 horsepower electric motor was chosen. This is a DC shunt wound motor (230 volts) with a control system comprised of solid state rectifiers and a motor driven variable transformer. The rated maximum continuous operating speed of the motor is 1750 RPM. To prevent the motor from taking up some of the room length and thereby shortening the flume, the motor was located beside the flume with a belt drive to a pulley on the propeller shaft located beneath a step built into the sump tank as shown in Figures 2 and 3. The nature of this arrangement permitted a speed reduction factor of 4 by use of different size pulleys on motor and impeller shaft leading to a maximum impeller RPM of 438.

Although we could have designed and constructed an impeller which was optimum for the flume, we first made an impeller from a standard 3-bladed ship propeller to test out the flume operation. The impeller was made from a 24-inch diameter by 16-inch pitch propeller with the outer radius turned down to 19.875 inches thus achieving wide blade tips with gaps of 1/16 inch between the tips and the nozzle wall. By making estimates from propeller charts, we concluded that with the available RPM range of 0 to 438, this impeller would drive the flume. However, at especially slow speeds, where the fluid advance speed is small but considerable impeller pressure is still needed to overcome the static head of the fluid in the upper branch of the flume, the impeller would be operating far from its optimum condition and some cavitation could be expected.

Diffuser. In order to expand the cross-sectional area of the flow from that at the impeller to that at the inlet to the contraction, a diffuser is needed somewhere in the flow

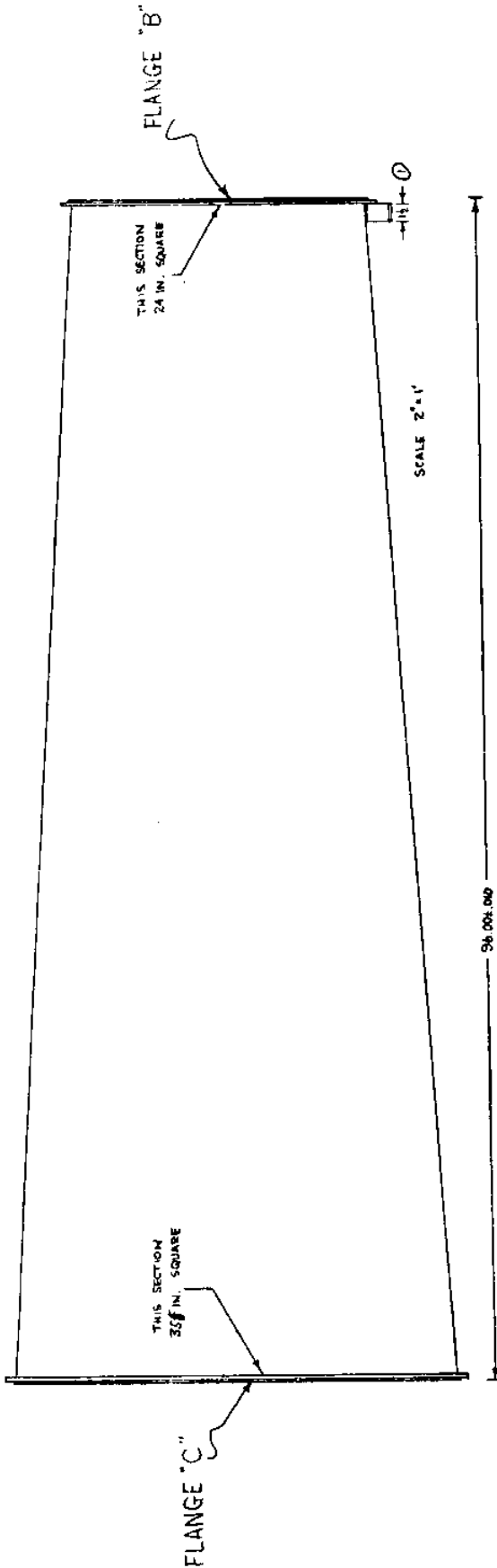
loop. The maximum contraction area ratio permitted by space limitations was about 4 so it was decided to expand the flow cross-sectional area in the diffuser to 3 feet by 3 feet. Since it was desirable to locate the contraction as close to the upstream end of the entire device as possible in order to maximize test section length, the diffuser was situated in the lower leg of the flume just downstream of the nozzle.

The diffuser was made with square cross sections and plane walls. A drawing of the diffuser is shown in Figure 10. At the upstream end the cross section is a 2 foot by 2 foot square and at the downstream end the cross section is a 3 foot by 3 foot square. The diffuser length is 8 feet.

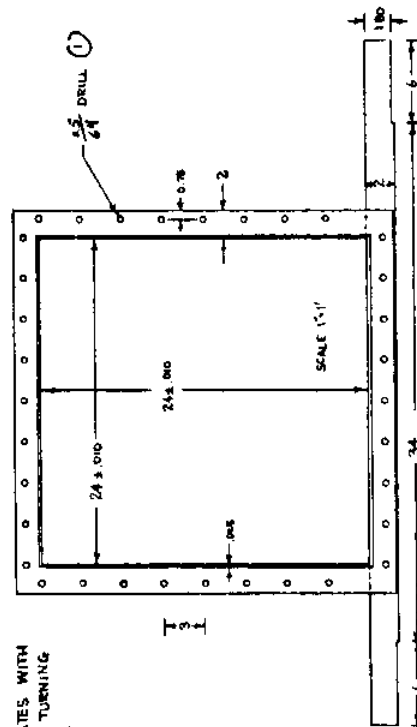
The diffuser was constructed by the same technique as was used to construct the nozzle. A male mold was made with the fiberglass diffuser laid up on top of the mold. The mold was then broken out of the diffuser after the resin had cured.

Turning Vane Section. The turning vane section is at one end of the flume and it contains two sets of turning vanes for turning the flow through 180° in going from the lower leg to the upper leg of the flume. Figure 11 shows a drawing of the turning vane section. This section was fabricated from stainless steel. A screen was installed between the flanges of the turning vane section and the diffuser. All screens had a construction of 17-by-17 meshes to the inch, constructed of a plain weave and 0.014-inch diameter stainless steel wire.

Stilling Section. A stilling section having a length of 1.92 feet was built and installed between the turning vane section and the contraction. Figure 12 shows a drawing of the stilling section. A screen was installed between the flanges of the turning vane section and the stilling section as was a screen between the flanges of the stilling section and the contraction. A bank of flow straightening tubes was installed in the stilling section. Each tube was 1 foot long, had a



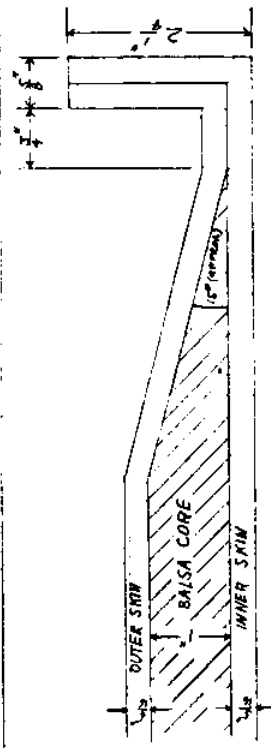
FLANGE "C" MATES WITH
FLANGE "D" IN TURNING
VANE SECTION.



SECTION ADJOINING FLANGE "B"
TO BE OF FIBERGLASS WITH STAINLESS
INSERT AT FLANGE. (1)

FABRICATOR PROVIDE 3/16" STAINLESS
PLATE DRILLED TO MATE WITH
FLANGE "B". (1)

CORE DETAILS AT FLANGES FOR FIBERGLASS CONSTRUCTION - FULL SCALE



NOTES FOR FIBERGLASS CONSTRUCTION - DIFFUSER AND NOZZLE

DRAWING IS FOR STEEL CONSTRUCTION - CHANGE TO FIBERGLASS 7-1-74
FOR FIBERGLASS, DO NOT DRILL FLANGES
FIBERGLASS TO BE OF BALSA CORE SANDWICH CONSTRUCTION WITH
5/16" THICK SKINS AND 1" CORE.
CORE THICKNESS TO BE TAPERED TO ZERO AT FLANGES AS
SHOWN ABOVE TO PREVENT INTERFERENCE WITH FLANGE BOLTS
INCREASE FLANGE WIDTH TO 2 1/2"
(1) IGNORE FOR FIBERGLASS CONSTRUCTION

(1) FLANGE "B"

MASSACHUSETTS INSTITUTE OF TECHNOLOGY
PRECISION FREE-SURFACE FLOW CHANNEL
DIFFUSER - RECTANGULAR SECTION
DIMENSIONS IN INCHES
DRAWN BY: W. B. LINCOLN
4 FEB. 1974

FIGURE 10. Flume Diffuser.

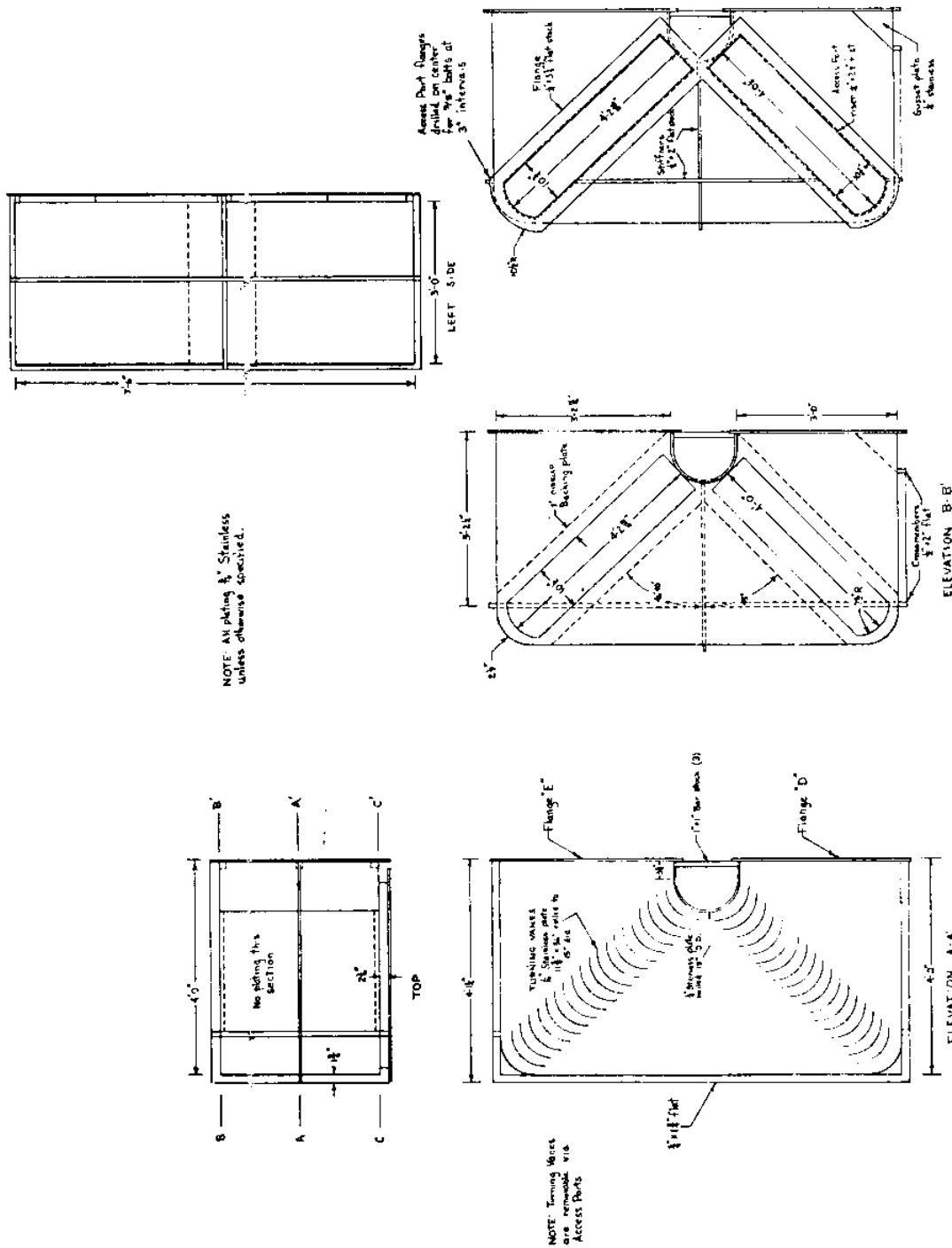


FIGURE 11. TURNING VANE SECTION.

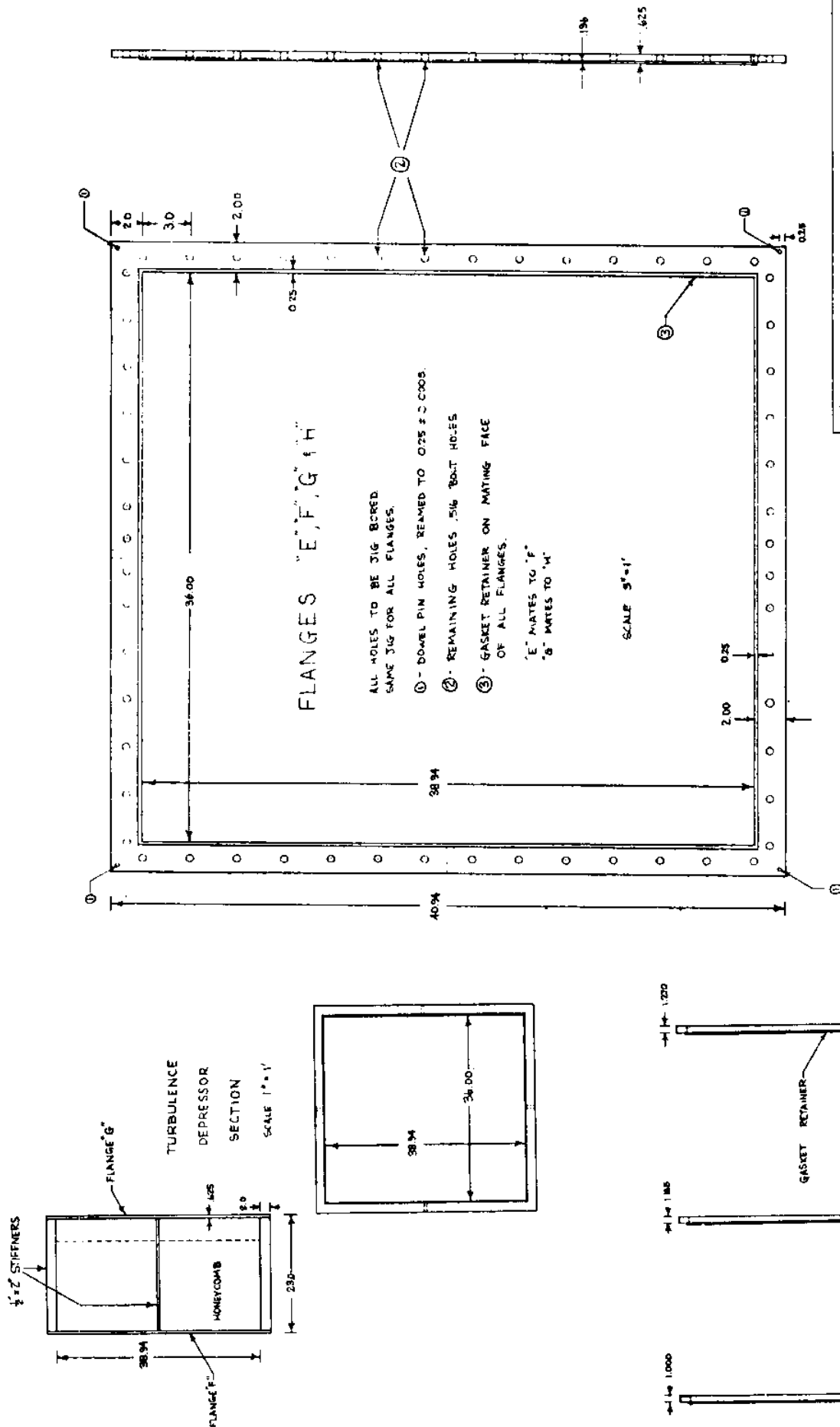


FIGURE 12. Stilling Section.

WEDGE INSERTS - BETWEEN FLANGES "G" & "H"
(SAME CROSS-SECTION AS FLANGE "G")

MASSACHUSETTS INSTITUTE OF TECHNOLOGY

PRECISION FREE-SURFACE FLOW CHANNEL

TURBULENCE DEPRESSOR SECTION, INSERTS & FLANGES

SAFETY IN ENGINEERING 1-A308

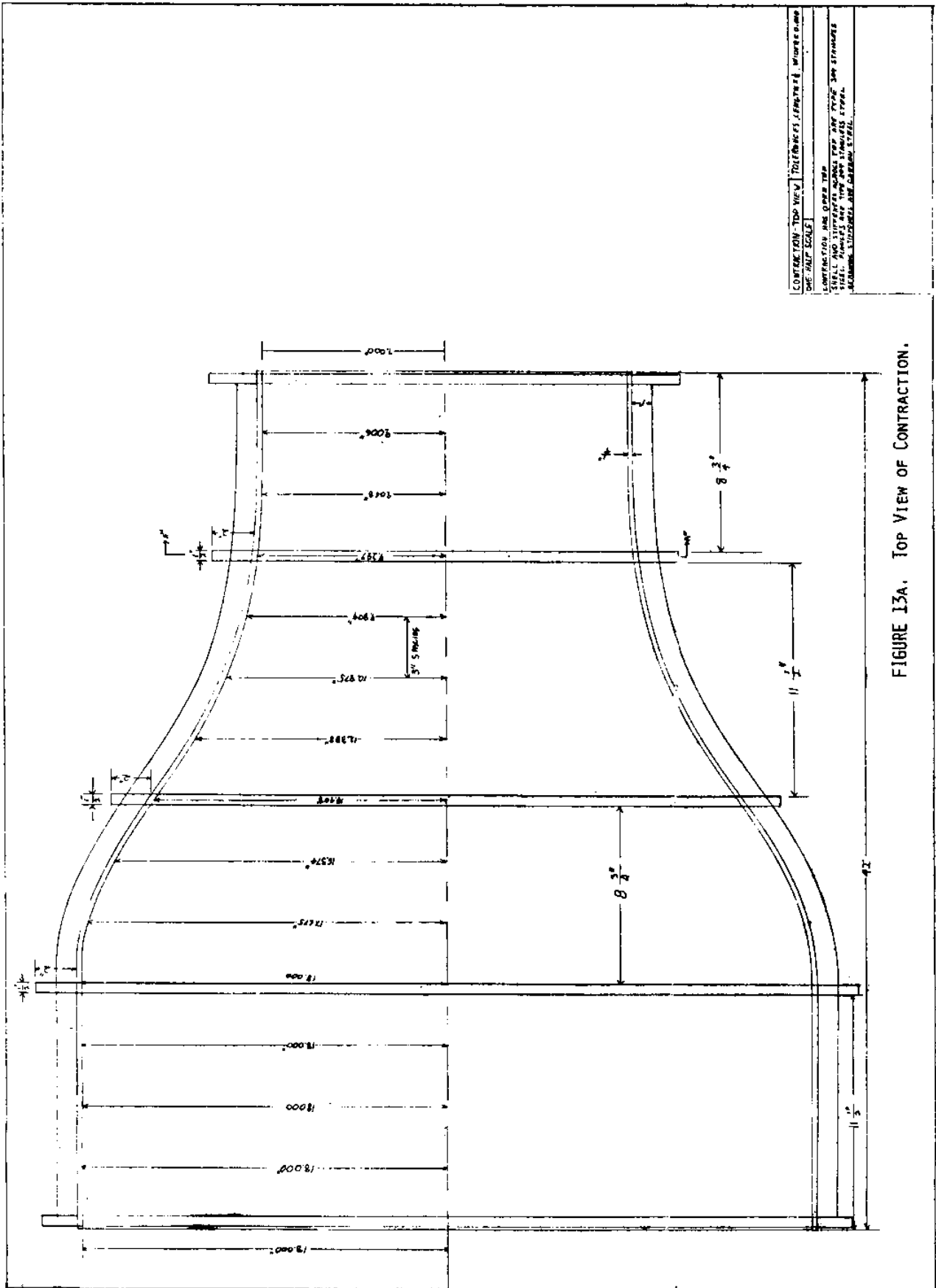
ALC AS NOTED

1-inch outside diameter, and a wall thickness of 0.037 inches. Both the stilling sections and the tubes were made of stainless steel. The tubes were close packed at the upstream end of the stilling section so that there was a gap between the downstream end of the tubes and the screen located between the stilling section and the contraction. The bank of tubes contained 43 horizontal rows with 35 tubes in each row, thus making 1,376 tubes in all. It was felt that the two cascades of turning vanes and the bank of tubes were sufficient to eliminate impeller-induced flow rotation so that anti-rotation vanes would not be necessary.

Contraction. Extensive design studies for contractions with square cross sections for flows without free surfaces has been done at M.I.T. (see Hanson, 1969). This has led to a basic contraction wall curve used both in the M.I.T. low noise acoustic wind tunnel and the M.I.T. variable pressure completely enclosed water tunnel; although the curve is scaled differently in each case to achieve different contraction ratios. In our flume model (MacDougal, 1974) we tested the same contraction wall curve shape on side and bottom walls using a free surface with natural draw down. This was found to be satisfactory for flume Froude numbers from 0 to 0.6. At higher Froude numbers waves would spring from the walls of the contraction and extend into the test section. This effect could be delayed to higher Froude numbers by making the contraction more gradual, but this would reduce available test section length. Since the satisfactory Froude number range was sufficient for the anticipated use, the same contraction shape was employed for the full scale flume. Figure 13 shows a drawing of the contraction.

4. OPERATIONAL TESTS

Flume Calibration. Two controls - impeller speed and the position of the combination weir - determine the operating condition of the oil layer flume, as defined by the height and





surface velocity of water in the test section. To expedite the use of the flume, a calibration was made whereby one can easily determine the operating condition which results from a given setting of the control variables. Weir position is defined arbitrarily by the height of the top edge of the weir plate with regard to its height when fully closed, i.e., when the bottom edge of the weir plate is resting on the bottom glass of the test section so that all of the flow is over the top of the plate. The fully closed position is weir position 1. Weir position 2 is defined to be that position where the top of the weir plate is 1 inch below its level in weir position 1, and other positions are defined similarly, in 1-inch increments. The other operator-controlled variable, impeller speed, is determined quite precisely by means of an electronic counter. Input to the counter is provided by a magnetic sensor located in such a way that it detects the passage of individual teeth of a 120-tooth gear which is mounted on the impeller shaft. Thus, the number of counts in a 1-second interval is twice the shaft RPM.

The height of water in the test section was measured by means of a transparent rule which was affixed to a glass side wall. The surface velocity, for purposes of calibration, was measured by timing the passage of floats along a known distance.

The calibration was performed with the sump tank filled at all times to the lowered sill between the sump and auxiliary tanks. Although the level of the water in the sump tank is an additional variable, no advantage was anticipated from running at less than the maximum height, while possible disadvantages include increased cavitation of the impeller, ventilation of the nozzle, and decreased time during which the water in the sump can rid itself of entrained oil and air.

The results of the calibration are shown in Figure 14. The curves were terminated at the left-hand side due to the

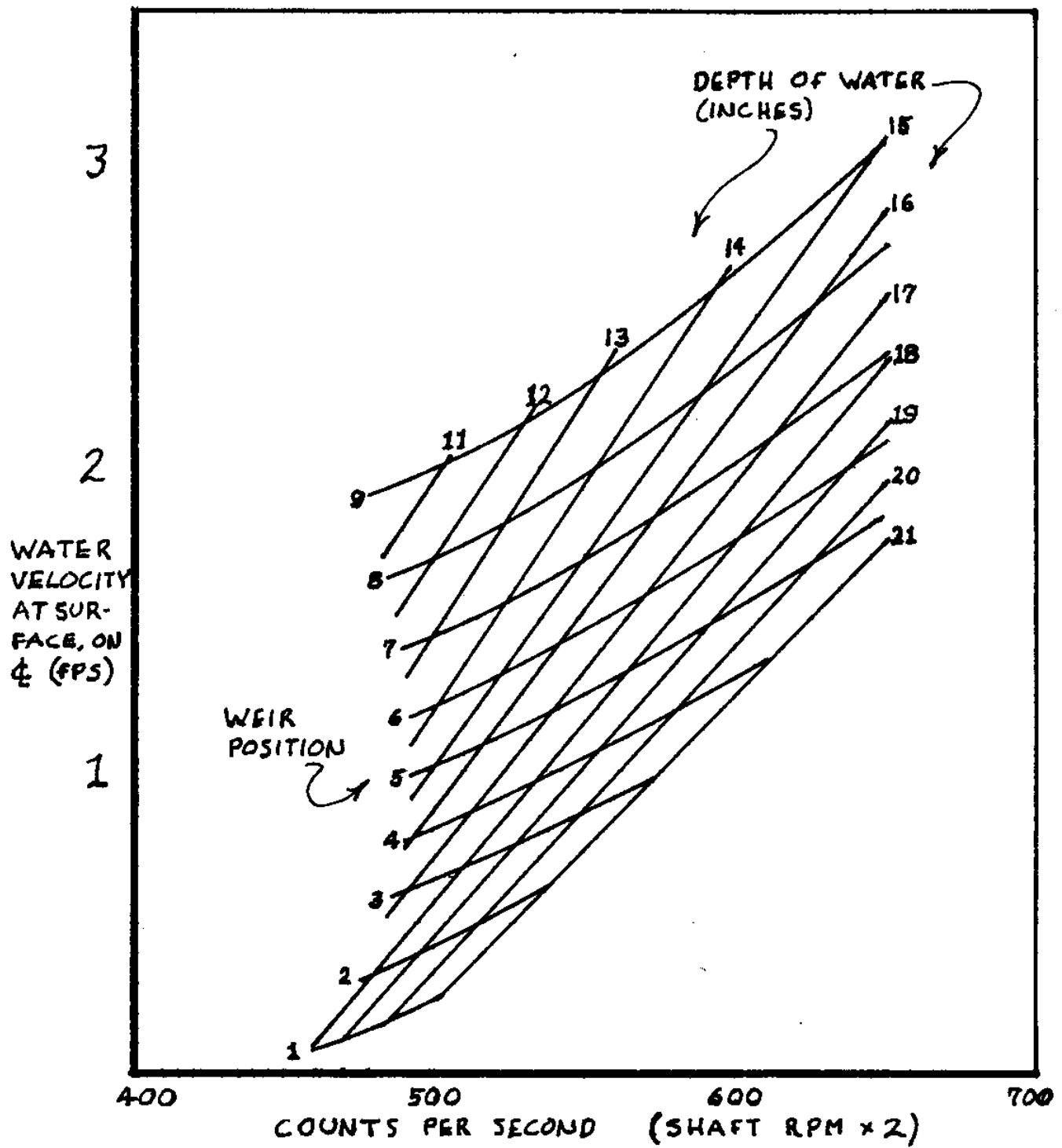


FIGURE 14. Water Surface Speed Calibration.

fact that the water level was no longer above the upper edge of the weir plate. In this condition, long period standing waves often occur, and the flow velocity and height become unsteady. On the right-hand side, the curves were terminated due to the fact that when continued beyond 325 RPM, they were no longer smooth. The cause for this was not determined. Data were not taken for water heights above 21 inches, since at this height the surface is no longer visible through the side glass. Data beyond weir position 9 were judged to be insufficiently precise due to the fixed length over which the floats could be timed.

Flow Uniformity. In order to investigate the uniformity of the flow, a velocity survey was taken near the beginning of the test section at two operating conditions - 1 ft/sec (18-inch water height) and 2.5 ft/sec (14-inch height). A Thermo-Systems 1050 Series constant-temperature anemometer (Models 1051-2D, 1054B and 1056) was used, equipped with a Model 1231W conical hot-film probe. Only one side of the test section was surveyed, since the flow was assumed to be symmetric. The results are shown in Figures 15 and 16. The largest velocity differences outside the boundary layers are on the order of 9%, the slowest flow being at the center of the free surface and the fastest near the lower corners of the test section. The reason for this nonuniformity probably lies in secondary flow phenomena. The trailing vortex sheets from the turning vanes could be responsible for setting up a circulation which sweeps boundary layer fluid to the outer boundary of the flow in the turning vane section. Were this flow nonuniformity not suppressed by the stilling section, it could still be apparent in the test section. A second source of secondary flow is the contraction, which would tend to bend sidewall vorticity and the vorticity causing the above mentioned nonuniformity in such a way as to once again sweep boundary

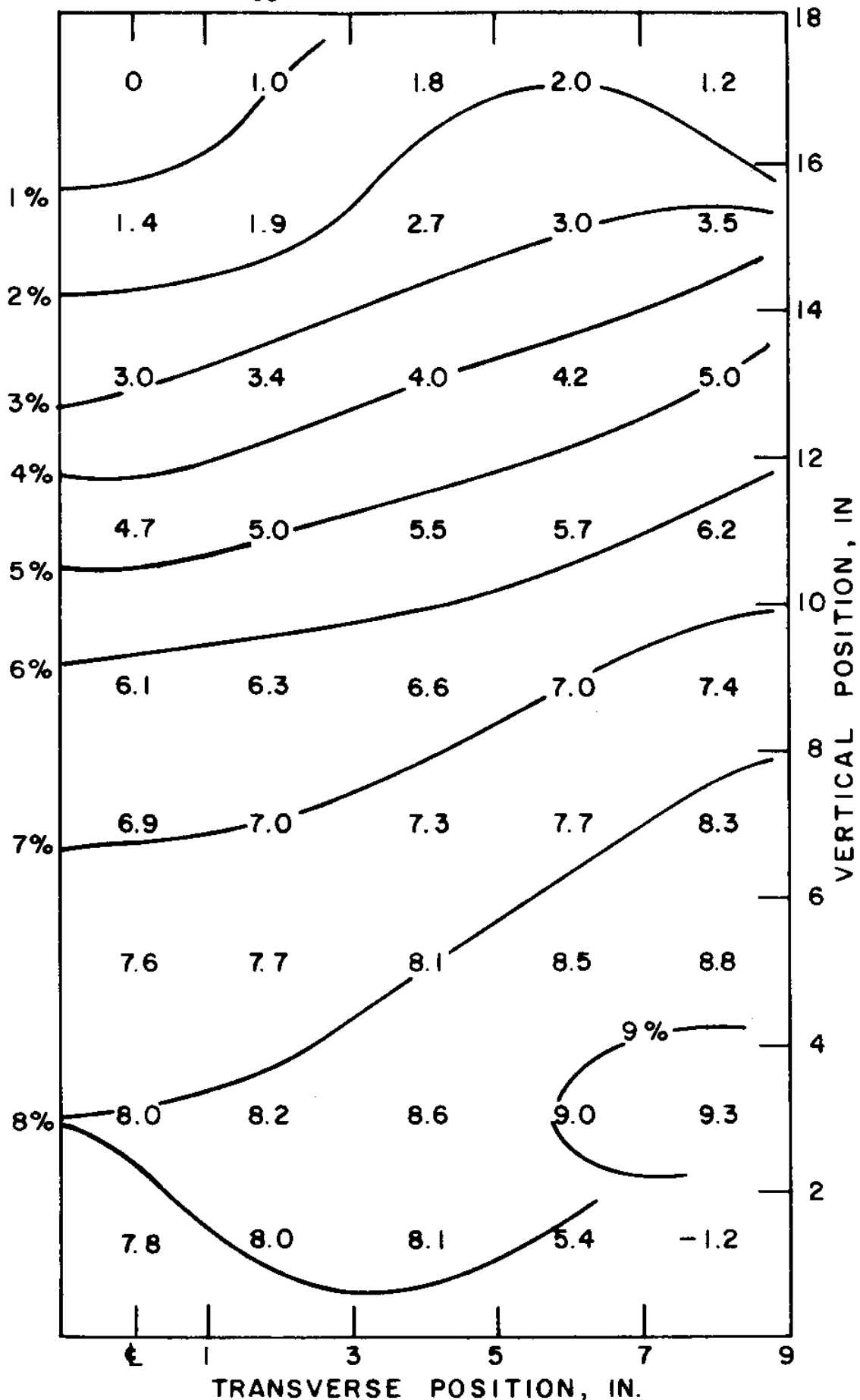


FIGURE 15. Survey of Flow Speed.
Percent above speed of surface along center plane of flume at a mean flow speed of 1 ft/sec (weir position 4; 540 counts/sec; measurements taken 27.5 inches from downstream end of contraction).

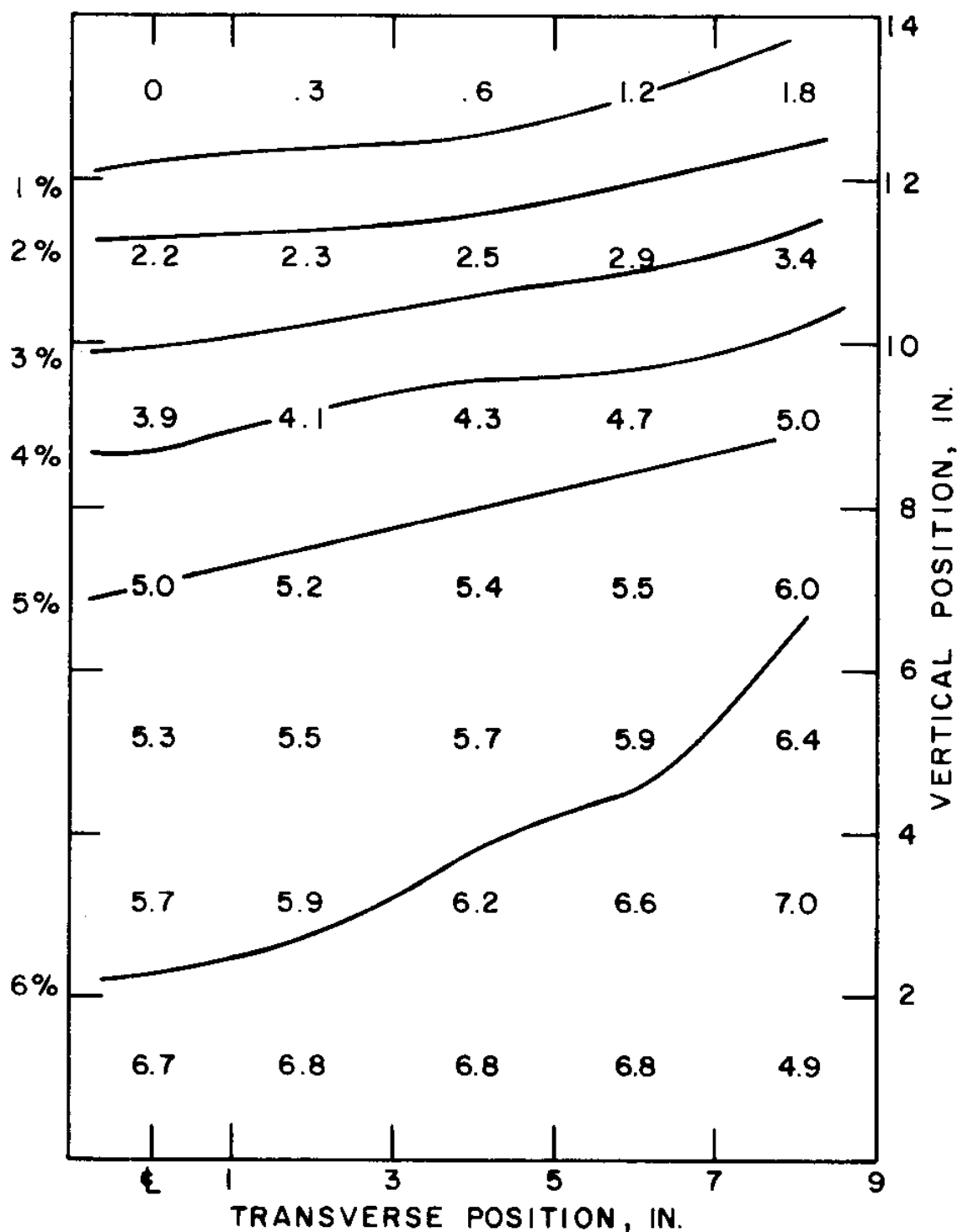


FIGURE 16. Survey of Flow Speed.
Percent above speed of surface along center plane of flume
at a mean flow speed of 2.5 ft/sec (weir position 9;
582 counts/sec; measurements taken 27.5 inches from
downstream end of contraction).

layer fluid to the top of the test section, and from there down along the centerline. By injecting dye into the test section at various points, it is possible to see such a secondary flow. A third source of secondary flow is that found in straight lengths of open channels and pipes of prismatic cross sections. All these flows tend to result in a velocity defect at the surface. Since the nonuniformity is apparent even quite near the contraction, it is judged unlikely that streamwise vorticity generated in the contraction or in the test section itself is responsible. It would seem that the stilling section does not completely smooth the flow from the turning vanes.

In order to correct the flow nonuniformity, it would be necessary to increase the solidity of the lower portion of the screen just upstream of the flow straightening tubes. Although this has not yet been accomplished, it is planned for the future.

Turbulence and Vibration Levels. Measurements of the longitudinal unsteady velocity on the centerplane of the test section 8 feet downstream from the contraction were taken at mean flow speeds of 0.5, 1.0, and 1.5 ft/sec. The measurements were made with the Thermo-Systems anemometer described above using a Thermo-Systems Model 1212-20W cylindrical hot-film probe and the resulting signal was high pass filtered at 0.1 Hz, squared, averaged with a 40 second time constant and then recorded. The square root of the recorded signal was taken as the rms of the longitudinal fluctuating velocity.

For the mean flow speed of 0.5 ft/sec, the rms of the unsteady velocity was nearly uniform with depth and approximately 2.2% of the mean stream speed. At the speeds of 1.0 and 1.5 ft/sec, the rms velocity fluctuations varied with depth, being approximately 2% of the mean stream speed near the free surface and about 1% of the mean stream speed over the lower portion of the test section.

The most likely cause of the higher fluctuating velocity near the free surface at the higher speeds is the nature of the flow near the free surface in the vicinity of the most downstream screen in the stilling section. The resistance of the screen causes the water level to be higher on the upstream side of the screen than on the downstream side. As a result, some water comes through the screen at a height which is above the downstream water level. This water actually drops onto the free surface with the impact generating considerable turbulence. As this turbulence region is convected downstream by the mean flow, it diffuses vertically so that the depth of the excessive turbulence region increases while the turbulence intensity decreases.

Apart from the 1% increase in the fractional apparent rms turbulence intensity caused by the above mentioned surface effect in the region of the measurements, we find rms longitudinal velocity fluctuations which are 2% of the mean stream speed for the .5 ft/sec flow and 1% of the mean stream speed for the 1.0 and 1.5 ft/sec flows. These mean speeds have a Reynolds number range which is small enough for one to expect the flume turbulence rms velocity to be a constant percentage of free stream speed. However, the measured rms velocity fluctuation percentage varies by a factor of 2. There is considerable evidence that this anomaly is due to the fact that the measured velocity fluctuations are due to the two independent processes of flume turbulence and flume vibration.

There is considerable vibration of the flume structure which can be felt by placing one's hand on the flume while it is operating; but quantitative measurements of vibration levels have not been made. The major source of vibration is the waterfall in the sump tank. Impeller cavitation is another source. The sensitivity of the hot film anemometer to vibratory fluid motion has been confirmed by other independent experiments we have performed.

In order to estimate the portion of the rms velocity fluctuations due to vibration and the portion of the rms velocity fluctuations due to turbulence, Figure 17 shows the measured rms velocity fluctuations (beneath the region influenced by the aforementioned free surface effect) as a function of flow speed. The figure also shows a straight line fit to these data. For velocity fluctuations proportional to flow speed, a straight line curve would result. Therefore, the longitudinal velocity fluctuations due to vibration can be estimated by the intercept of the straight line with the ordinate of the graph and the turbulence intensity can be estimated by the slope of the line. This yields the results that the estimate of the longitudinal velocity fluctuations related to vibration are 0.008 ft/sec and the estimate of the turbulence level in the flume below the surface region is 0.4% of the free stream speed. In the vicinity of the free surface, the turbulence intensity is somewhat higher. The increase in near-surface turbulence intensity varies from zero at low speeds to approximately 1% of the free stream speed at a speed of 1.5 ft/sec.

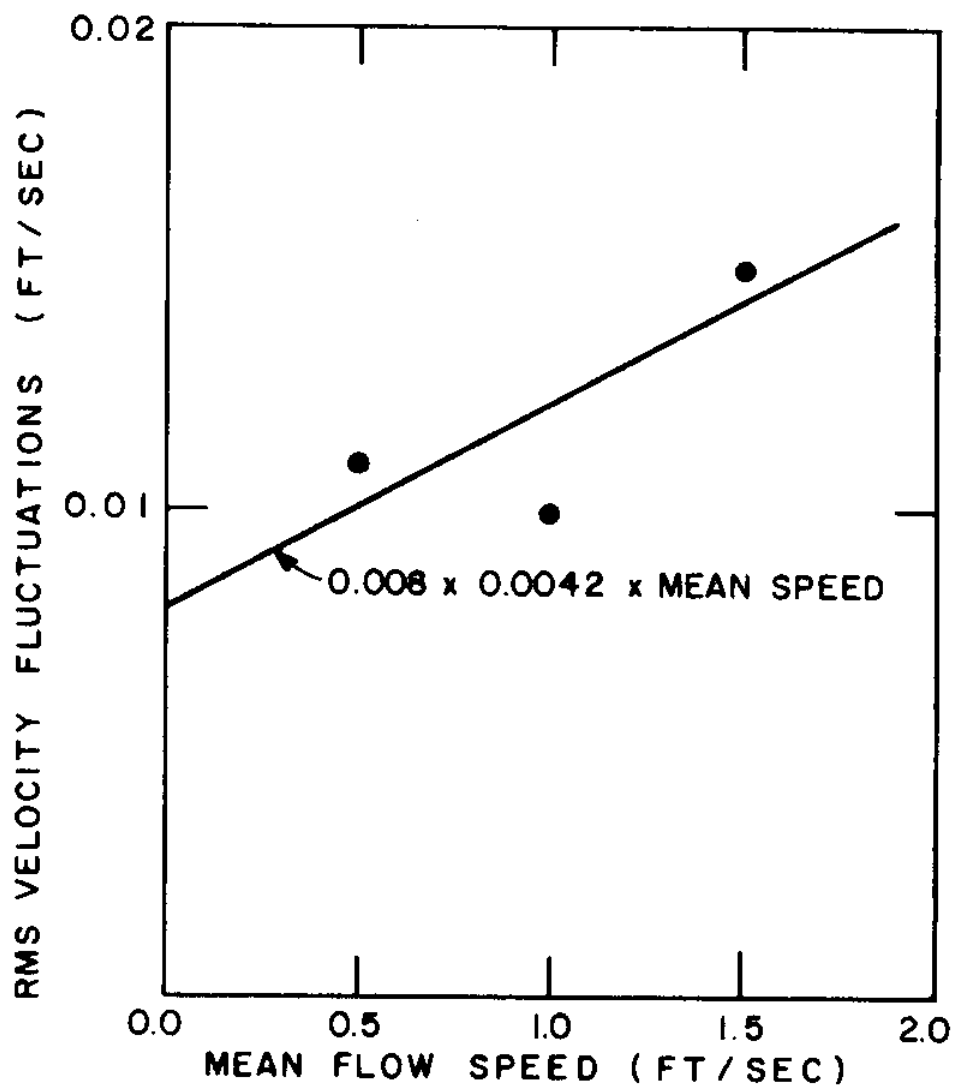


FIGURE 17. RMS Velocity Fluctuations Versus Mean Flow Speed Beneath Free Surface Effects.

- Measurements
- Straight line fit through data

REFERENCES

- (1) Hale, L.A., Norton, D.J., and Rodenberger, C.A., 1974, "The Effect of Currents and Waves on an Oil Slick Retained by a Barrier," U.S. Coast Guard Report No. CG-D-53-75.
- (2) Hanson, Carl E., 1969, "The Design and Construction of a Low-noise, Low-turbulence Wind Tunnel, M.I.T. Engineering Projects Laboratory Report No. DSR 79611-1.
- (3) MacDougal, R.E., 1974, "Development of a Precision Low Speed Flume," S.M. Thesis, M.I.T., Department of Ocean Engineering.
- (4) Miller, E., Lindenmuth, W., and Altman, R., 1972, "Analysis of Lightweight Oil Containment System Sea Trials," Hydro-nautics, Incorporated, Technical Report 7220-1.
- (5) Nelson, S.B., 1976, "Water Engineering," in Standard Handbook for Civil Engineers, 2nd ed., Merritt, F.S. (ed.), McGraw-Hill Book Company.
- (6) Orkney, J.C., 1955, "The Development of a Hydraulic Flume for Ship Model Testing," Brit. Ship. Res. Assoc. Rep. No. 1965.
- (7) Preston, J.H., 1966, "The Design of High Speed Free Surface Water Channels," Proceedings of NATO Advanced Study Institute on 'Surface Hydrodynamics,' Bressanone.
- (8) Steele, B.N., 1962, "A Design Study of a Circulating Water Channel," National Physical Laboratory Report S.H. R26/62.

